

End-to-end guarantees for indirect data-driven control of bilinear systems with finite stochastic data [★]

Nicolas Chatzikiriakos, Robin Strässer, Frank Allgöwer, Andrea Iannelli

University of Stuttgart, Institute for Systems Theory and Automatic Control, 70550 Stuttgart, Germany

Abstract

In this paper we propose an end-to-end algorithm for indirect data-driven control for bilinear systems with stability guarantees. We consider the case where the collected i.i.d. data is affected by probabilistic noise with possibly unbounded support and leverage tools from statistical learning theory to derive finite sample identification error bounds. To this end, we solve the bilinear identification problem by solving a set of linear and affine identification problems, by a particular choice of a control input during the data collection phase. We provide a priori as well as data-dependent finite sample identification error bounds on the individual matrices as well as ellipsoidal bounds, both of which are structurally suitable for control. Further, we integrate the structure of the derived identification error bounds in a robust controller design to obtain an exponentially stable closed loop. By means of an extensive numerical study, we showcase the interplay between the controller design and the derived identification error bounds. Moreover, we note appealing connections of our results to indirect data-driven control of general nonlinear systems through Koopman operator theory and discuss how our results may be applied in this setup.

Key words: Bilinear Systems, Finite Sample Identification, Indirect Data-Driven Control, Statistical Learning Theory

1 Introduction

Bilinear systems are an important class of nonlinear systems that naturally appears across different domains such as biological processes (Mohler et al., 1980), socioeconomics (Mohler, 1973) but also in engineering, e.g., nuclear reactor dynamics (Mohler, 1973) and thermal control processes such as building control (Underwood, 2002). Further, the class of bilinear systems has recently received great attention for its ability to represent nonlinear systems through a higher-dimensional lifting, e.g., Carleman linearization or Koopman operator theory (Mauroy et al., 2020; Surana, 2016; Huang et al., 2018). Due to the wide-ranging occurrences of bilinear systems, there is significant interest in learning the behavior of a bilinear sys-

tem from data. However, currently there are only very few methods that allow to analyze the identification error from a finite-sample perspective. Such finite-sample results are of particular importance when it comes to indirect data-driven control of bilinear systems, where the identified system model is used to control the real system. Since usually only finite data can be collected and this data is often affected by noise, it is important to account for the introduced uncertainty to obtain end-to-end guarantees.

Related works There exists a rich literature in classical system identification for both linear and nonlinear systems (Ljung, 1998). The special case of bilinear systems has received considerable interest since many of the techniques used in linear system identification can be carried over to the bilinear setting (Fnaiech and Ljung, 1987). In particular, Favoreel et al. (1999) generalize linear subspace identification to the bilinear setting under the assumption of white noise excitation. Further, Berk Hizir et al. (2012) reduce the bilinear identification problem to the identification of an equivalent linear model by choosing suitable sinusoidal inputs. The problem of persistency of excitation and input selection for the identification of bilinear systems has been considered, e.g., by Dasgupta et al. (1989) and Sontag et al. (2009).

Note that the previously discussed classical system identification literature only provides asymptotic results in

[★] This work is funded by Deutsche Forschungsgemeinschaft (DFG, German Research Foundation) under Germany's Excellence Strategy - EXC 2075 – 390740016 and within grant AL 316/15-1 – 468094890. We acknowledge the support by the Stuttgart Center for Simulation Science (SimTech). N. Chatzikiriakos and R. Strässer thank the Graduate Academy of the SC SimTech for its support.

Email address:
 nicolas.chatzikiriakos@ist.uni-stuttgart.de (Nicolas Chatzikiriakos), robin.straesser@ist.uni-stuttgart.de (Robin Strässer), frank.allgower@ist.uni-stuttgart.de (Frank Allgöwer), andrea.iannelli@ist.uni-stuttgart.de (Andrea Iannelli).

the presence of stochastic noise, i.e., results that consider the case where the number of data collected goes to infinity. Building on recent advances in high dimensional statistics (Wainwright, 2019; Abbasi-Yadkori et al., 2011), first finite-sample system identification results have recently emerged for linear time-invariant (LTI) and certain classes of nonlinear systems. For LTI systems, where the ordinary least squares (OLS) estimator is predominantly used, Dean et al. (2020) provide individual identification error bounds for the unknown system matrices assuming that the available data is independent. Correlation in trajectory data is handled by Simchowitz et al. (2018) using the block martingale small-ball condition. Allowing for dependent data comes at the cost of being restricted to marginally stable systems and not recovering individual identification error bounds on the unknown matrices. While the stability assumption is overcome in the works of Shirani Faradonbeh et al. (2018) and Sarkar and Rakhlin (2019), finding individual error bounds for each of the matrices from trajectory data is still an open problem. Extending the LTI literature, Foster et al. (2020) and Sattar and Oymak (2022) provide a finite-sample identification analysis for generalized linear systems with a known nonlinearity. When it comes to bilinear systems, Sattar et al. (2022) establish finite-sample identification error bounds for data collected from a single trajectory. However, their derived bound relies on a potentially restrictive stability assumption and comes in the form of a single upper bound of the identification errors for all the identified system matrices. Sattar et al. (2025) extend previous works on bilinear systems by providing a finite sample identification analysis for partially observed bilinear systems. Since we can only provide a brief overview of the field of non-asymptotic system identification, we refer to Tsiamis et al. (2023) and Ziemann et al. (2023) for more detailed discussions.

Despite the interest in applying statistical learning theory tools to bound identification errors, there have been comparably less works using the finite-sample error bounds for a robust controller design. One important reason for this is that the bounds are often not directly usable for a (robust) controller design, and therefore providing end-to-end guarantees for an indirect data-driven control scheme may be difficult. For the linear-quadratic regulator, Dean et al. (2020) establish an indirect data-driven control scheme with end-to-end guarantees. In the work of Mania et al. (2019) this analysis is improved. Further, Tsiamis et al. (2022) provide upper and lower bounds on the sample complexity of stabilizing LTI systems using indirect data-driven control.

While these developments provide valuable insights into the theoretical limits of *linear* indirect data-driven control, they do not address corresponding extensions to bilinear systems. For this class of systems, there exists a rich literature on model-based controller designs, including Lyapunov-based methods (Pedrycz, 1980; Derese and Noldus, 1980), bang-bang control with linear switching policy (Longchamp, 1980), quadratic state

feedback (Gutman, 1981, 1980), nonlinear state feedback (Benallou et al., 1988), constant feedback (Luesink and Nijmeijer, 1989), or schemes for passive bilinear systems (Lin and Byrnes, 1994). Moreover, Huang and Jadbabaie (1999) propose to view the state of bilinear systems as a scheduling variable, which leads to a convex controller design using results for (quasi-)linear parameter-varying systems. Another approach is to use linear matrix inequalities (LMIs) to design controllers for bilinear systems in a local region, see, e.g., Amato et al. (2009) for a polytopic region and Khlebnikov (2018) for an ellipsoidal region, or Coutinho et al. (2019) for input-delayed systems. Relying on robust control techniques, closed-loop stability guarantees for bilinear systems are derived in Strässer et al. (2023) using an LMI-based controller in a pre-defined region, while Strässer et al. (2025a) design a globally stabilizing controller based on sum-of-squares (SOS) optimization. However, most of the available results require model knowledge or are restricted to noise-free systems.

Contribution In this work, we consider the problem of identifying a bilinear system from noisy data to control the underlying system with end-to-end guarantees. Specifically, we leverage tools from statistical learning theory to enable robust control of bilinear systems using collected data. First, we present novel finite-sample error bounds for identifying bilinear systems from finite i. i. d. data. Here, we use the control input to solve a set of linear and affine identification problems in order to identify the bilinear system from data. We note that the novel finite-sample analysis of affine identification problems might be of independent interest. Since the corresponding OLS solutions do no longer depend on purely random matrices we leverage properties of symmetric matrices to analyze the random part and the determinist parts of the corresponding matrices separately. Combining this with (anti-)concentration inequalities allows us to provide high-probability identification error bounds. We not only present a priori identification error bounds revealing the structural dependencies on key problem parameters, but also data-dependent identification error bounds that prove to be less conservative. Compared to Sattar et al. (2022), where finite-sample identification error bounds from trajectory data are provided, the identification error bounds derived in this work are structurally tailored to indirect data-driven control. This enables combining the identification error bound with robust control approaches for bilinear systems. More precisely, we provide an easy-to-use algorithm to derive an indirect data-driven controller along with closed-loop stability guarantees. To the best of our knowledge, this is the first work providing such an end-to-end result for finite data affected by stochastic noise with possibly unbounded support in the case of bilinear systems. Further, we show that the proposed results may be applicable beyond bilinear systems through the Koopman operator and note appealing connections to Koopman-based indirect data-driven control of more general classes of nonlinear systems. Finally, we showcase the

effectiveness of the results in several numerical investigations, where we demonstrate the interplay between the controller design and the derived error bounds.

Outline This paper is structured as follows. Section 2 introduces the problem setup including the considered bilinear systems. In Section 3, we derive finite-sample identification error bounds for bilinear systems. Then, we use the obtained bounds for the design of indirect data-driven controllers guaranteeing closed-loop exponential stability of bilinear systems in Section 4. Finally, we illustrate the effectiveness of the derived identification error bounds in comparison to Monte Carlo simulations as well as in the controller design in Section 5, before concluding the paper in Section 6.

Notation The unit sphere in \mathbb{R}^n is denoted by \mathbb{S}^{n-1} . For a positive scalar $c \in \mathbb{R}_{>0}$ we denote a sphere centered around the origin of \mathbb{R}^n with radius c by $c\mathbb{S}^{n-1}$. Given a matrix A , we denote the spectral norm by $\|A\|_2$. The operation $[a]_i$ extracts the i -th element of the vector a or the i -th column when applied to a matrix. We denote matrix blocks that can be inferred from symmetry by \star , i.e., we write $\Lambda^\top \Sigma \Lambda = [\star]^\top \Sigma \Lambda$. By \otimes we denote the Kronecker product. Further, we write $X \sim \mathcal{N}(\mu, \Sigma)$ if the random vector $X \in \mathbb{R}^{n_x}$ is Gaussian distributed with mean μ and covariance Σ . We write $Y \sim \text{subG}(\sigma^2)$ if the random variable $Y \in \mathbb{R}$ is zero-mean sub-Gaussian with variance proxy σ^2 . Moreover, we write $X \sim \text{subG}_{n_x}(\sigma^2)$ if the random vector $X \in \mathbb{R}^{n_x}$ is zero-mean sub-Gaussian with variance proxy σ^2 , that is if the one-dimensional marginals $\langle X, v \rangle$ are zero-mean sub-Gaussian random variables with variance proxy σ^2 for all $v \in \mathbb{S}^{n_x-1}$. Finally, $Y \sim U(a)$ and $Y \sim \text{subExp}(\nu^2, \alpha)$ denote a random variable $Y \in \mathbb{R}$ which is uniformly distributed on $[-a, a]$ and sub-exponential with parameters (ν^2, α) , respectively.

2 Problem setup

We consider an unknown bilinear system of the form

$$x_t^+ = Ax_t + B_0 u_t + \sum_{i=1}^{n_u} [u_t]_i A_i x_t + w_t, \quad (1)$$

where $w_t \stackrel{\text{i.i.d.}}{\sim} \text{subG}_{n_x}(\sigma_w^2)$ is unknown process noise, $x_t, x_t^+ \in \mathbb{R}^{n_x}$ are the state vector at the current time step t and the next time step, respectively, and $u_t \in \mathbb{R}^{n_u}$ is a control input. Note that by defining $B_i := A_i + A$, the system (1) can be equivalently described by

$$x_t^+ = Ax_t + B_0 u_t + \sum_{i=1}^{n_u} [u_t]_i (B_i - A) x_t + w_t \quad (2a)$$

$$= Ax_t + B_0 u_t + A_{ux} (u_t \otimes x_t) + w_t, \quad (2b)$$

where $A_{ux} = [B_1 - A \cdots B_{n_u} - A]$. We consider an indirect data-driven control scheme which consists of two steps. First we identify the unknown matrices $A \in \mathbb{R}^{n_x \times n_x}$, $B_0 \in \mathbb{R}^{n_x \times n_u}$, $B_1, \dots, B_{n_u} \in \mathbb{R}^{n_x \times n_x}$ from data and characterize the uncertainty regions for the estimates. Second, we deploy a robust control scheme

accounting for the identification error to obtain a data-driven controller with end-to-end guarantees.

The structure in (2) can be leveraged to reduce the nonlinear identification problem of identifying the bilinear system (2) to $n_u + 1$ linear identification problems. To this end, we conduct $n_u + 1$ experiments in which we choose the constant control inputs $u_t \equiv u^0 := 0$ and $u_t \equiv u^i := e_i$ for $i \in [1, n_u]$, respectively, where e_i are the elements of the canonical basis of \mathbb{R}^{n_u} and i is the index of the experiment. This yields the $n_u + 1$ system descriptions

$$\mathcal{S}_0 : \quad x_t^+ = Ax_t + w_t, \quad (3a)$$

$$\mathcal{S}_i : \quad x_t^+ = Ax_t + [B_0]_i + (B_i - A)x_t + w_t \\ = [B_0]_i + B_i x_t + w_t, \quad \forall i = 1, \dots, n_u, \quad (3b)$$

describing the behavior of the unknown bilinear system (2) under the respective control inputs. In the following, we consider the problem of identifying $\mathcal{S}_0, \dots, \mathcal{S}_{n_u}$ which, as shown previously, is equivalent to identifying the bilinear system (2).

Remark 1 We choose the canonical basis $\{e_1, \dots, e_{n_u}\}$ as inputs for simplicity. Particularly, any other basis $\{v_1, \dots, v_{n_u}\}$ of \mathbb{R}^{n_u} could be chosen in addition to the zero input. Clearly, there exists an invertible matrix H that maps between the two bases, i.e., $v_i = He_i$ for all $i \in [1, n_u]$. Applying the input $u_t \equiv v_i$ to the system (2) results in

$$\begin{aligned} x_t^+ &= Ax_t + B_0 v_i + A_{ux}(v_i \otimes x_t) \\ &= Ax_t + B_0 He_i + A_{ux}(He_i \otimes x_t) \\ &= Ax_t + B_0 He_i + A_{ux}(He_i \otimes I_{n_x})x_t. \end{aligned}$$

Defining $\tilde{B}_i = A_{ux}(He_i \otimes I_{n_x}) + A$ and $\tilde{B}_0 = B_0 H$ yields $x_t^+ = \tilde{B}_i x_t + [\tilde{B}_0]_i$, i.e., a structurally identical identification problem to (3b). Understanding the effect of the selected basis on the accuracy of identification and subsequently on the data-driven control scheme is an interesting direction for future work.

To solve the linear and affine identification problems (3), we resort to the OLS estimator to obtain finite sample guarantees. To this end, we collect T_i samples from \mathcal{S}_i for each $i \in [0, n_u]$, where the number of samples will be specified in our analysis. Identifying the autonomous LTI system (3a) from finite data has already been considered, see, e.g., Matni and Tu (2019) for a detailed analysis. However, the finite-sample identification of the affine system (3b) is yet unsolved and is the main technical challenge for obtaining finite sample identification error bounds tailored to control. More precisely, the robust controller design requires identification error bounds which are proportional to the state and input. For this reason, we seek finite sample identification error bounds that hold for all the unknown matrices individually, hence named individual identification error bounds hereafter. Obtaining individual, a priori identification error bounds from correlated data is an open problem in literature even in the case of linear systems (Ziemann et al., 2023). To address this, we restrict the sampling according to the following assumption.

Algorithm 1 Proposed identification algorithm

Require: Sampling scheme

```

for  $i \in [0, n_u]$  do
  Choose input  $u^i$ 
  for  $t \leq T_i$  do
    Sample state  $x_t$  according to sampling scheme
    Evaluate bilinear system with  $x_t$  and  $u^i$ 
  end for
end for
Compute OLS estimates for (3)

```

Assumption 2 For each of the realizations \mathcal{S}_i , $i \in [0, n_u]$, the data is obtained by sampling according to $x_t \stackrel{i.i.d.}{\sim} \text{subG}_{n_x}(\sigma_x^2)$.

Note that, although potentially restrictive in practical applications, independence of the data is key for the proposed individual bounds. However, assuming the same distribution for each \mathcal{S}_i is without loss of generality and the distribution can be selected to meet specified requirements. In practice, Assumption 2 can be satisfied by collecting the data from multiple trajectories. Specifically, the data can be collected by rolling out the unforced system for some time before applying u^i to the system for one time step. Then the procedure is repeated by starting a new trajectory at the origin. Using this approach, which is similar to approaches proposed by Dean et al. (2020); Matni and Tu (2019), the requirements for data collection can be satisfied by using the endpoints from multiple trajectories. In fact, the trajectory (and, thus, correlated) data collected from the unforced system can be used to learn the matrix A , where the bounds derived in, e.g., Simchowitz et al. (2018) can be used if A is marginally stable.

Remark 3 Compared to the works of Dean et al. (2020); Matni and Tu (2019) which rely on Gaussian noise and sampling, the extension to sub-Gaussian sampling allows for more correlations inside the sampled state vector. As a consequence, the constants in the burn-in time conditions are larger, but this more general analysis paves the way for applications in Koopman-based control (Section 3.4).

Algorithm 1 summarizes the proposed identification procedure, where the deployed sampling scheme is determined depending on the desired error bounds.

3 Finite sample identification error bounds

Next, we present high probability finite sample identification error bounds for each of the unknown elements in (3) in order to identify the bilinear system (2). In particular, we use the OLS estimator to identify the true system parameters from data. To this end, we define

$$\theta_i := \begin{bmatrix} B_i & [B_0]_i \end{bmatrix} \quad \forall i \in [1, n_u], \quad y_t := \begin{bmatrix} x_t^\top & 1 \end{bmatrix}^\top$$

such that the OLS estimator is given by

$$\hat{A} \in \arg \min_A \sum_{t=1}^{T_0} \|x_t^+ - Ax_t\|_2^2, \quad (4a)$$

$$\hat{\theta}_i \in \arg \min_{\theta_i} \sum_{t=1}^{T_i} \|x_t^+ - \theta_i y_t\|_2^2 \quad \forall i \in [1, n_u]. \quad (4b)$$

Further, we introduce the normalized regressors

$$\xi_t := \frac{x_t}{\sigma_x} \stackrel{\text{i.i.d.}}{\sim} \text{subG}_{n_x}(1), \quad \zeta_t := \begin{bmatrix} \xi_t^\top & 1 \end{bmatrix}^\top \quad (5)$$

and, with slight abuse of notation, define

$$X := \begin{bmatrix} \xi_1 & \xi_2 & \cdots & \xi_{T_i} \end{bmatrix}^\top, \quad Y := \begin{bmatrix} \zeta_1 & \zeta_2 & \cdots & \zeta_{T_i} \end{bmatrix}^\top, \\ X^+ := \begin{bmatrix} x_1^+ & x_2^+ & \cdots & x_{T_i}^+ \end{bmatrix}^\top, \quad W := \begin{bmatrix} w_0 & w_1 & \cdots & w_{T_i} \end{bmatrix}^\top.$$

Then, the closed-form solutions to (4) read

$$\hat{A}^\top = \frac{1}{\sigma_x} (X^\top X)^{-1} (X^\top X^+), \quad (6a)$$

$$\hat{\theta}_i^\top = \begin{bmatrix} \frac{1}{\sigma_x} & 0 \\ 0 & 1 \end{bmatrix} (Y^\top Y)^{-1} (Y^\top X^+), \quad \forall i \in [1, n_u]. \quad (6b)$$

Defining the normalized empirical covariance matrices

$$M_0 := \sum_{t=1}^{T_0} \xi_t \xi_t^\top, \quad M_i := \begin{bmatrix} \sum_{t=1}^{T_i} \xi_t \xi_t^\top & \sum_{t=1}^{T_i} \xi_t \\ \sum_{t=1}^{T_i} \xi_t^\top & T_i \end{bmatrix} \quad (7)$$

for all $i \in [1, n_u]$ leads to the identification errors

$$(\hat{A} - A)^\top = \frac{1}{\sigma_x} M_0^{-1} (X^\top W), \quad (8a)$$

$$(\hat{\theta}_i - \theta_i)^\top = \begin{bmatrix} \frac{1}{\sigma_x} & 0 \\ 0 & 1 \end{bmatrix} M_i^{-1} (Y^\top W), \quad \forall i \in [1, n_u]. \quad (8b)$$

The identification error (8a) has been previously analyzed for Gaussian noise, e.g., by Matni and Tu (2019). Next, we extend the result to sub-Gaussian noise and sampling.

Theorem 4 Consider the autonomous system (3a). Fix a failure probability $\delta \in (0, 1)$ and let the data $\{x_t^+, x_t\}_{t=1}^{T_0}$ be collected according to Assumption 2. If

$$T_0 \geq 128 \log(8 \cdot 9^{n_x} / \delta), \quad (9)$$

then the identification error (8a) of the OLS estimate (6a) is bounded by

$$\|\hat{A} - A\|_2 \leq \frac{\sigma_w}{\sigma_x} \frac{16 \sqrt{T_0 \log(4 \cdot 9^{n_x} / \delta)}}{T_0} \quad (10)$$

with probability at least $1 - \frac{\delta}{2}$.

PROOF. First, using sub-multiplicativity of the norm, (8a) yields

$$\|\hat{A} - A\|_2 \leq \frac{1}{\sigma_x} \frac{\|X^\top W\|}{\lambda_{\min}(M_0)}.$$

Then, we apply Propositions 15 and 16 (Appendix A) with $\frac{\delta}{4}$ and $c = \frac{1}{4}$ to obtain the result. \square

In the following, we use tools from Vershynin (2012) and Wainwright (2019) to derive a priori and data-dependent upper bounds on the identification error in (8b).

3.1 A priori identification error bounds

First, we provide novel a priori identification error bounds, which reveal fundamental dependencies on key parameters, e.g., the problem size or the desired confidence for the affine identification problem (3b).

Theorem 5 *Consider the unknown system \mathcal{S}_i as defined in (3b) for any $i \in [1, n_u]$. Fix a failure probability $\delta \in (0, 1)$ and let the data $\{x_t^+, x_t\}_{t=1}^{T_i}$ be collected according to Assumption 2. If*

$$T_i \geq 64(3 + 2\sqrt{2}) \log(8n_u 9^{n_x} / \delta),$$

then the identification error (8b) of the OLS estimate (6b) is bounded by

$$\|(\hat{B}_i - B_i)\|_2 \leq \frac{\sigma_w}{\sigma_x} \frac{\frac{4\sqrt{10}}{3} \sqrt{2T_i \log(4n_u 9^{n_x} / \delta)}}{T_i/2 - \frac{4}{3} \sqrt{2T_i \log(4n_u 9^{n_x} / \delta)}},$$

$$\|([\hat{B}_0]_i - [B_0]_i)\|_2 \leq \sigma_w \frac{\frac{4\sqrt{10}}{3} \sqrt{2T_i \log(4n_u 9^{n_x} / \delta)}}{T_i/2 - \frac{4}{3} \sqrt{2T_i \log(4n_u 9^{n_x} / \delta)}},$$

with probability at least $1 - \frac{\delta}{2n_u}$.

PROOF. While this proof is structured similar to the proof of LTI finite sample identification results (see, e.g., Matni and Tu (2019)), there are some key differences owing to the difficulties introduced by the affine structure in (3b). Importantly, the regressor y_t is not purely random. Thus, the matrix M_i defined in (7) is not a purely random matrix and, hence, cannot be handled using the existing arguments. Analyzing these partially random quantities will pose the main technical difficulty.

Since we are interested in individual error bounds of B_i and $[B_0]_i$, we observe that

$$(\hat{B}_i - B_i)^\top = \begin{bmatrix} I_{n_x} & 0_{n_x \times 1} \end{bmatrix} (\hat{\theta}_i - \theta_i)^\top$$

$$([\hat{B}_0]_i - [B_0]_i)^\top = \begin{bmatrix} 0_{1 \times n_x} & 1 \end{bmatrix} (\hat{\theta}_i - \theta_i)^\top.$$

Exploiting (8b) results in the individual error bounds

$$(\hat{B}_i - B_i)^\top = \begin{bmatrix} \frac{1}{\sigma_x} I_{n_x} & 0_{n_x \times 1} \end{bmatrix} M_i^{-1} Y^\top W, \quad (12a)$$

$$([\hat{B}_0]_i - [B_0]_i)^\top = \begin{bmatrix} 0_{1 \times n_x} & 1 \end{bmatrix} M_i^{-1} Y^\top W. \quad (12b)$$

Now, we take the norm of (12) and use submultiplicativity of the matrix norm to obtain

$$\|\hat{B}_i - B_i\|_2 \leq \frac{1}{\sigma_x} \frac{\|Y^\top W\|_2}{\lambda_{\min}(M_i)}, \quad (13a)$$

$$\|[\hat{B}_0]_i - [B_0]_i\|_2 \leq \frac{\|Y^\top W\|_2}{\lambda_{\min}(M_i)}, \quad (13b)$$

where $\lambda_{\min}(M_i)$ denotes the smallest eigenvalue of the matrix M_i . We split the analysis of the terms on the right-hand side into the analysis of the smallest eigenvalue of M_i and controlling the norm in the numerator.

Controlling the smallest eigenvalue of M_i . Since M_i is not a purely random matrix we need to deploy different tools than the ones presented in Matni and Tu (2019) to

control $\lambda_{\min}(M_i)$. In particular, we proceed in two steps. First, we show that we can express the smallest eigenvalue of the full matrix as the smallest eigenvalue of the block diagonal terms and an error term depending on the off-diagonal elements. Then, we use Hoeffding's inequality to show that the off-diagonal elements are small compared to the block-diagonal terms if we collect enough samples. For the subsequent analysis we apply the Courant-Fisher minimax theorem (Golub and Van Loan, 2013, Theorem 8.1.2) and consider $v \in \mathbb{R}^{n_x+1}$ with $\|v\| = 1$, such that we obtain

$$\begin{aligned} \lambda_{\min}(M_i) &= \min_{v \in \mathbb{S}^{n_x}} \begin{bmatrix} v_1^\top \\ v_2^\top \end{bmatrix} \begin{bmatrix} \sum_{t=1}^{T_i} \xi_t \xi_t^\top & \sum_{t=1}^{T_i} \xi_t \\ \sum_{t=1}^{T_i} \xi_t^\top & T_i \end{bmatrix} \begin{bmatrix} v_1 \\ v_2 \end{bmatrix} \\ &= \min_{v \in \mathbb{S}^{n_x}} v_1^\top \left(\sum_{t=1}^{T_i} \xi_t \xi_t^\top \right) v_1 + 2v_2 v_1^\top \sum_{t=1}^{T_i} \xi_t + v_2^2 T_i \\ &\geq \min_{v \in \mathbb{S}^{n_x}} v_1^\top \left(\sum_{t=1}^{T_i} \xi_t \xi_t^\top \right) v_1 + v_2^2 T_i - 2|v_2| \left| v_1^\top \sum_{t=1}^{T_i} \xi_t \right|. \end{aligned}$$

Note that we can combine the first two terms into an eigenvalue condition on a block-diagonal matrix, i.e.,

$$\begin{aligned} \lambda_{\min}(M_i) &\geq \lambda_{\min} \left(\begin{bmatrix} \sum_{t=1}^{T_i} \xi_t \xi_t^\top & 0 \\ 0 & T_i \end{bmatrix} \right) \\ &\quad - \max_{v \in \mathbb{S}^{n_x}} 2|v_2| \left| v_1^\top \sum_{t=1}^{T_i} \xi_t \right|. \end{aligned} \quad (14)$$

More precisely, (14) shows that the minimum eigenvalue of the block-diagonal matrix as well as the error term serve as a lower-bound on the true minimum eigenvalue.

We first derive an upper bound on the term $\max_{v \in \mathbb{S}^{n_x}} 2|v_2| \left| v_1^\top \sum_{t=1}^{T_i} \xi_t \right|$. To this end, note that $\|v\|_2 = 1$ which implies $\|v_1\|_2^2 + |v_2|^2 = 1$. Defining $\bar{v}_1 = \frac{1}{\sqrt{1-v_2^2}} v_1$ yields $\bar{v}_1 \in \mathbb{S}^{n_x-1}$. Hence, we rewrite

$$\max_{v \in \mathbb{S}^{n_x}} 2|v_2| \left| v_1^\top \sum_{t=1}^{T_i} \xi_t \right| = \max_{\substack{v_2 \in [-1, 1] \\ \bar{v}_1 \in \mathbb{S}^{n_x-1}}} 2|v_2| \sqrt{1 - v_2^2} \left| \bar{v}_1^\top \sum_{t=1}^{T_i} \xi_t \right|,$$

where we can maximize over \bar{v}_1 and v_2 separately. Thus, we use Lemma 17 (Appendix A) with $\frac{\delta}{4n_u}$ to obtain

$$\begin{aligned} \max_{v \in \mathbb{S}^{n_x}} 2|v_2| \left| v_1^\top \sum_{t=1}^{T_i} \xi_t \right| &\leq \max_{v_2 \in [-1, 1]} \frac{4}{3} |v_2| \sqrt{1 - v_2^2} \sqrt{2T_i \log(4n_u \cdot 9^{n_x} / \delta)} \\ &= \frac{2}{3} \sqrt{2T_i \log(4n_u \cdot 9^{n_x} / \delta)} \end{aligned}$$

with probability at least $1 - \frac{\delta}{4n_u}$. Here, the last step follows by plugging in the maximizer

$$v_2^* = \arg \max_{v_2 \in [-1, 1]} |v_2| \sqrt{1 - v_2^2} = \frac{1}{\sqrt{2}}.$$

Now, we consider

$$\lambda_{\min} \left(\begin{bmatrix} \sum_{t=1}^{T_i} \xi_t \xi_t^\top & 0 \\ 0 & T_i \end{bmatrix} \right) = \min \left\{ \lambda_{\min} \left(\sum_{t=1}^{T_i} \xi_t \xi_t^\top \right), T_i \right\}.$$

Then, we use Proposition 16 (Appendix A) to obtain

$$\mathbb{P} \left[\lambda_{\min} \left(\sum_{t=1}^{T_i} \xi_t \xi_t^\top \right) \geq T_i (1 - 2c)^2 \right] \geq 1 - \frac{\delta}{4n_u},$$

where $c \in (0, \frac{1}{2})$. Thus,

$$\lambda_{\min}(M_i) \geq T_i (1 - 2c)^2 - \frac{4}{3} \sqrt{2T_i \log(4n_u 9^{n_x} / \delta)} \quad (15)$$

with probability at least $\left(1 - \frac{\delta}{4n_u}\right) \left(1 - \frac{\delta}{4n_u}\right) \geq 1 - \frac{\delta}{2n_u}$ if $T_i \geq \frac{8}{c^2} \log(8n_u 9^{n_x} / \delta)$. To ensure that (15) yields a non-trivial bound (and the inverses in (13) exist), we need to impose the additional condition

$$T_i (1 - 2c)^2 - \frac{4}{3} \sqrt{2T_i \log(8n_u 9^{n_x} / \delta)} > 0$$

which is satisfied if $T_i > \frac{32}{9(1-2c)^4} \log(8n_u 9^{n_x} / \delta)$. We select $c = \frac{\sqrt{2}-1}{2\sqrt{2}}$, which yields

$$\lambda_{\min}(M_i) \geq \frac{T_i}{2} - \frac{4}{3} \sqrt{2T_i \log(4n_u 9^{n_x} / \delta)} \quad (16)$$

with probability at least $1 - \frac{\delta}{2n_u}$ if

$$\begin{aligned} T_i &> \max \left\{ \frac{128}{9}, 64(3 + 2\sqrt{2}) \right\} \log(8n_u 9^{n_x} / \delta) \\ &= 64(3 + 2\sqrt{2}) \log(8n_u 9^{n_x} / \delta). \end{aligned}$$

Controlling the noise term. To handle the numerator in (13), consider that

$$\begin{aligned} \|Y^\top W\|_2 &= \sup_{\substack{u \in \mathbb{S}^{n_x} \\ v \in \mathbb{S}^{n_x-1}}} \sum_{t=1}^{T_i} \left(u^\top \begin{bmatrix} \xi_t \\ 1 \end{bmatrix} \right) (w_t^\top v) \\ &= \sup_{\substack{u \in \mathbb{S}^{n_x} \\ v \in \mathbb{S}^{n_x-1}}} \sum_{t=1}^{T_i} (u_1^\top \xi_t + u_2) (w_t^\top v) \\ &= \sup_{\substack{u \in \mathbb{S}^{n_x} \\ v \in \mathbb{S}^{n_x-1}}} \sum_{t=1}^{T_i} (u_1^\top \xi_t) (w_t^\top v) + u_2 (w_t^\top v). \end{aligned}$$

Using similar techniques as in the analysis of (14) and introducing $\bar{u}_1 = \frac{1}{\sqrt{1-u_2^2}} u_1$ leads to

$$\begin{aligned} \|Y^\top W\|_2 &= \sup_{\substack{v \in \mathbb{S}^{n_x-1} \\ \bar{u}_1 \in \mathbb{S}^{n_x-1} \\ u_2 \in [-1, 1]}} \sum_{t=1}^{T_i} \sqrt{1 - u_2^2} (\bar{u}_1^\top \xi_t) (w_t^\top v) + u_2 (w_t^\top v) \\ &\leq \sup_{u_2 \in [-1, 1]} \left[\sqrt{1 - u_2^2} \sup_{\substack{v \in \mathbb{S}^{n_x-1} \\ \bar{u}_1 \in \mathbb{S}^{n_x-1}}} \left| \sum_{t=1}^{T_i} (\bar{u}_1^\top \xi_t) (w_t^\top v) \right| \right. \\ &\quad \left. + |u_2| \sup_{v \in \mathbb{S}^{n_x-1}} \left| \sum_{t=1}^{T_i} w_t^\top v \right| \right]. \quad (17) \end{aligned}$$

Observe that

$$\sup_{\substack{v \in \mathbb{S}^{n_x-1} \\ \bar{u}_1 \in \mathbb{S}^{n_x-1}}} \left[\sum_{t=1}^{T_i} (\bar{u}_1^\top \xi_t) (w_t^\top v) \right] = \left\| \sum_{t=1}^{T_i} \xi_t w_t^\top \right\|_2,$$

i.e., we can apply Proposition 15 (Appendix A) with $\frac{\delta}{4n_u}$ to obtain that if $T_i \geq \frac{1}{2} \log(4n_u 9^{2n_x} / \delta)$, then

$$\sup_{\substack{v \in \mathbb{S}^{n_x-1} \\ \bar{u}_1 \in \mathbb{S}^{n_x-1}}} \left[\sum_{t=1}^{T_i} (\bar{u}_1^\top \xi_t) (w_t^\top v) \right] \leq 4\sigma_w \sqrt{T_i \log(4n_u 9^{2n_x} / \delta)} \quad (18)$$

holds with probability at least $1 - \frac{\delta}{4n_u}$. Further, we use Lemma 17 (Appendix A) to deduce the upper bound

$$\sup_{v \in \mathbb{S}^{n_x-1}} \left| v^\top \sum_{t=1}^{T_i} w_t \right| \leq \frac{4}{3} \sigma_w \sqrt{2T_i \log(4n_u 9^{n_x} / \delta)} \quad (19)$$

with probability at least $1 - \frac{\delta}{4n_u}$. Union bounding (18) and (19) and plugging the result into (17) leads to

$$\begin{aligned} \|Y^\top W\|_2 &\leq \sup_{u_2 \in [-1, 1]} \sqrt{1 - u_2^2} 4\sigma_w \sqrt{T_i \log(4n_u 9^{2n_x} / \delta)} \\ &\quad + |u_2| \frac{4}{3} \sigma_w \sqrt{2T_i \log(4n_u 9^{n_x} / \delta)} \\ &\leq \sup_{u_2 \in [-1, 1]} \sqrt{1 - u_2^2} 4\sigma_w \sqrt{2T_i \log(4n_u 9^{n_x} / \delta)} \\ &\quad + |u_2| \frac{4}{3} \sigma_w \sqrt{2T_i \log(4n_u 9^{n_x} / \delta)} \\ &= \sup_{u_2 \in [-1, 1]} 4\sigma_w \sqrt{2T_i \log(4n_u 9^{n_x} / \delta)} \left(\sqrt{1 - u_2^2} + \frac{|u_2|}{3} \right) \end{aligned}$$

with probability at least $1 - \frac{\delta}{2n_u}$ if $T_i \geq \frac{1}{2} \log(4n_u 9^{2n_x} / \delta)$. Finally, plugging in the maximizer $u_2^* = \frac{1}{\sqrt{10}}$ yields

$$\|Y^\top W\|_2 \leq \frac{4\sqrt{10}}{3} \sigma_w \sqrt{2T_i \log(4n_u 9^{n_x} / \delta)}. \quad (20)$$

Combining the previous results. Taking (16) and (20), plugging them into (13), and using union bound arguments leads to the desired result. Further, we compare the two burn-in time conditions

$$\begin{aligned} \max \left\{ \frac{1}{2} \log(4n_u 9^{2n_x} / \delta), 64(3 + 2\sqrt{2}) \log(8n_u 9^{n_x} / \delta) \right\} \\ = 64(3 + 2\sqrt{2}) \log(8n_u 9^{n_x} / \delta) \quad \forall n_x, n_u \geq 1 \end{aligned}$$

which concludes the proof. \square

Note that like in the LTI case assuming i. i. d. data allows us to provide error bounds on the individual matrices independently of the stability properties of the system considered. Further, the bounds in Theorem 5 can be computed *before* collecting data, relying only on knowledge of the system dimensions and the noise variance.

3.2 Data-dependent identification error bounds

Depending on the application it might not be necessary to provide a priori identification error bounds, i.e., before data collection. Instead, one can turn to data-dependent error bounds that account only for the data observed and, hence, are less conservative. To this end, recall the matrices M_i defined in (7) and note that they can be evaluated from data, i.e., we do not need to control the respective inverses. Thus, we can leverage the derivations from the previous section to obtain individual bounds for each of the unknown matrices.

Corollary 6 *Consider the unknown system \mathcal{S}_i as defined in (3b) for any $i \in [1, n_u]$. Fix a failure probability $\delta \in (0, 1)$ and let the data $\{x_t^+, x_t\}_{t=1}^{T_i}$ be collected according to Assumption 2. If $T_i \geq \frac{1}{2} \log(2n_u 9^{2n_x} / \delta)$, then the identification error of the OLS estimate (6b) satisfies*

$$\begin{aligned} \|(\hat{B}_i - B_i)\|_2 &\leq \frac{\sigma_w}{\sigma_x} \frac{\frac{4\sqrt{10}}{3} \sqrt{2T_i \log(2n_u \cdot 9^{n_x} / \delta)}}{\lambda_{\min}(M_i)}, \\ \|(\hat{B}_0)_i - [B_0]_i\|_2 &\leq \sigma_w \frac{\frac{4\sqrt{10}}{3} \sqrt{2T_i \log(2n_u \cdot 9^{n_x} / \delta)}}{\lambda_{\min}(M_i)} \end{aligned}$$

with probability at least $1 - \frac{\delta}{2n_u}$, where the matrix M_i is defined in (7). If M_i has zero as an eigenvalue, we define the inverse of that eigenvalue to be infinity.

Alternatively, we can use similar proof techniques to (Dean et al., 2020, Proposition 3) to obtain ellipsoidal, data-dependent identification error bounds.

Lemma 7 *Consider the unknown system \mathcal{S}_i as defined in (3b) for any $i \in [1, n_u]$ and with $w_t \stackrel{i.i.d.}{\sim} \mathcal{N}(0, \sigma_w^2 I_{n_x})$. Fix a failure probability $\delta \in (0, 1)$ and let the data $\{x_t^+, x_t\}_{t=1}^{T_i}$ be sampled i. i. d. with $T_i \geq n_x + 1$. Define*

$$C_1(n_x, \delta) = \sigma_w^2 \left(\sqrt{n_x + 1} + \sqrt{n_x} + \sqrt{2 \log(2n_u / \delta)} \right)^2.$$

Then, with probability at least $1 - \frac{\delta}{2n_u}$, we have

$$[\star] \begin{bmatrix} (\hat{B}_i - B_i)^\top \\ ([\hat{B}_0]_i - [B_0]_i)^\top \end{bmatrix}^\top \preceq C_1(n_x, \delta) \begin{pmatrix} [\star]^\top M_i \begin{bmatrix} \frac{1}{\sigma_x} & 0 \\ 0 & 1 \end{bmatrix}^{-1} \end{pmatrix}.$$

If M_i has zero as an eigenvalue, we define the inverse of that eigenvalue to be infinity.

PROOF. We only provide a short version of the proof, for a more detailed version we refer to the proof of (Matni and Tu, 2019, Proposition V.1). First, define

$$\tilde{Y}^\top = \begin{bmatrix} \frac{1}{\sigma_x} & 0 \\ 0 & 1 \end{bmatrix} Y^\top \quad (22)$$

and $E^\top = [(\hat{B}_i - B_i) \ ([\hat{B}_0]_i - [B_0]_i)]$. Assuming $T_i \geq n_x + 1$, the singular value decomposition of \tilde{Y} is given by $\tilde{Y} = U \Lambda V^\top$. Hence, if the inverse of Λ exists, we obtain

$$EE^\top = V \Lambda^{-1} U^\top W W^\top U \Lambda^{-1} V^\top \preceq \|U^\top W\|_2^2 (\tilde{Y}^\top \tilde{Y})^{-1}.$$

Each element of the matrix $U^\top W \in \mathbb{R}^{(n_x+1) \times n_x}$ is i. i. d. $\mathcal{N}(0, \sigma_w^2)$ and, thus, we apply (Vershynin, 2012, Corollary 5.35) to show $\|U^\top W\|_2 \leq \sigma_w (\sqrt{n_x + 1} + \sqrt{n_x} + \sqrt{2 \log(2n_u / \delta)})$ with probability at least $1 - \frac{\delta}{2n_u}$. \square

Note that, Lemma 7 only requires the data to be sampled i.i.d. but does not pose any additional requirements on the sampling distribution. This provides same additional flexibility that can be leveraged in practice. Lemma 7 can be straightforwardly extended to sub-Gaussian noise using (Vershynin, 2012, Proposition 5.39) instead of (Vershynin, 2012, Corollary 5.35).

3.3 Sample complexity of identifying bilinear systems

To obtain finite sample identification error bounds for the bilinear system (2), we apply Algorithm 1 and combine the results from Sections 3.1 and 3.2 using union bound arguments.

Theorem 8 *Consider Algorithm 1 with data collected from the bilinear system (2) according to Assumption 2. Fix a failure probability $\delta \in (0, 1)$. If*

$$T_0 \geq \bar{T}_0 \quad \text{and} \quad T_i \geq \bar{T}_i \quad \forall i \in [1, n_u],$$

then Algorithm 1 results in estimates $\hat{A}, \hat{B}_0, \hat{B}_1, \dots, \hat{B}_{n_u}$ that satisfy

$$\|\hat{A} - A\|_2 \leq \varepsilon_A, \quad (23a)$$

$$\|\hat{B}_i - B_i\|_2 \leq \varepsilon_{B_i} \quad \forall i \in [1, n_u], \quad (23b)$$

$$\|(\hat{B}_0)_i - [B_0]_i\|_2 \leq \varepsilon_{[B_0]_i} \quad \forall i \in [1, n_u] \quad (23c)$$

with probability at least $1 - \delta$, where identification error bounds and burn-in times are specified as follows:

(1) *A priori identification error bounds:*

$$\varepsilon_A = \frac{\sigma_w}{\sigma_x} \frac{16\sqrt{T_0 \log(4 \cdot 9^{n_x} / \delta)}}{T_0}, \quad (24a)$$

$$\varepsilon_{B_i} = \frac{\sigma_w}{\sigma_x} \frac{\frac{4\sqrt{10}}{3} \sqrt{2T_i \log(4n_u 9^{n_x} / \delta)}}{T_i/2 - \frac{4}{3} \sqrt{2T_i \log(4n_u 9^{n_x} / \delta)}}, \quad (24b)$$

$$\varepsilon_{[B_0]_i} = \frac{\sigma_w}{T_i/2 - \frac{4}{3} \sqrt{2T_i \log(4n_u 9^{n_x} / \delta)}} \frac{\frac{4\sqrt{10}}{3} \sqrt{2T_i \log(4n_u 9^{n_x} / \delta)}}{T_i/2 - \frac{4}{3} \sqrt{2T_i \log(4n_u 9^{n_x} / \delta)}}, \quad (24c)$$

$$\bar{T}_0 = 128 \log(8 \cdot 9^{n_x} / \delta), \quad (24d)$$

$$\bar{T}_i = 64(3 + 2\sqrt{2}) \log(8n_u 9^{n_x} / \delta). \quad (24e)$$

(2) *Data-dependent identification error bounds:*

$$\varepsilon_A = \frac{\sigma_w}{\sigma_x} \frac{4\sqrt{T_0 \log(4 \cdot 9^{n_x} / \delta)}}{\lambda_{\min}(M_0)}, \quad (25a)$$

$$\varepsilon_{B_i} = \frac{\sigma_w}{\sigma_x} \frac{\frac{4\sqrt{10}}{3} \sqrt{2T_i \log(2n_u \cdot 9^{n_x} / \delta)}}{\lambda_{\min}(M_i)}, \quad (25b)$$

$$\varepsilon_{[B_0]_i} = \frac{\sigma_w}{\lambda_{\min}(M_i)} \frac{\frac{4\sqrt{10}}{3} \sqrt{2T_i \log(2n_u 9^{n_x} / \delta)}}{\lambda_{\min}(M_i)}, \quad (25c)$$

$$\bar{T}_0 = \frac{1}{2} \log(2 \cdot 9^{n_x} / \delta), \quad (25d)$$

$$\bar{T}_i = \frac{1}{2} \log(2n_u 9^{2n_x} / \delta). \quad (25e)$$

PROOF. This result follows directly by using Theorem 5 (Corollary 6) and (the data-dependent version of) Theorem 4 and leveraging union bound arguments. \square

While we observe in Section 5.1 that the a priori identification error bounds (24) are less tight than the data-dependent identification ones (25), they provide the possibility to bound the amount of uncertainty in the estimates before running the experiment. Further, the a priori identification error bounds provide additional insights that help to understand the difficulty in identifying the system matrices in terms of the sample complexity. First, we can observe that the identification of every unknown matrix scales with $\mathcal{O}(1/\sqrt{T})$ which is the known rate of OLS for linear systems. Further, the problem size influences the identification errors (24a)-(24c) of order $\mathcal{O}(\sqrt{n_x \log(n_u)})$, whereas the overall number of samples $T = T_0 + n_u T_i$ needs to be of order $\mathcal{O}(n_x(n_u + 1))$. In accordance with the linear case, the failure probability enters inversely inside log-terms and lastly, we observe the signal-to-noise ratio (SNR) σ_x/σ_w for the identification error bounds of A and B_i , $\forall i \in [1, n_u]$, whereas the identification error of $[B_0]_i$ lacks the dependence on σ_x . This is because $[B_0]_i$ enters affinely in (3b), i.e., the sampling variance does not influence the rate of identifying $[B_0]_i$.

Equivalently, we can use the ellipsoidal, data-dependent identification error bounds to obtain the following result.

Theorem 9 Consider Algorithm 1 with i. i. d. data collected from the bilinear system (2). Fix a failure probability $\delta \in (0, 1)$ and let $w_t \stackrel{i.i.d.}{\sim} \mathcal{N}(0, \sigma_w^2 I_{n_x})$. If

$$T_0 \geq n_x \quad \text{and} \quad T_i \geq n_x + 1 \quad \forall i \in [1, n_u],$$

then Algorithm 1 results in estimates $\hat{A}, \hat{B}_0, \hat{B}_1, \dots, \hat{B}_{n_u}$ that satisfy

$$(\hat{A} - A)^\top (\hat{A} - A) \preceq \mathcal{E}_A, \quad (26a)$$

$$[\star] \left[\begin{array}{c} (\hat{B}_i - B_i)^\top \\ ([\hat{B}_0]_i - [B_0]_i)^\top \end{array} \right]^\top \preceq \mathcal{E}_{B_i} \quad \forall i \in [1, n_u] \quad (26b)$$

with probability at least $1 - \delta$, where

$$\begin{aligned} \mathcal{E}_A &= \frac{\sigma_w^2}{\sigma_x^2} \left(2\sqrt{n_x} + \sqrt{2 \log(2/\delta)} \right)^2 M_0^{-1}, \\ \mathcal{E}_{B_i} &= \sigma_w^2 \left(\sqrt{n_x + 1} + \sqrt{n_x} + \sqrt{2 \log(2n_u/\delta)} \right)^2 \\ &\quad \cdot \left(\begin{bmatrix} \sigma_x I_{n_x} & 0 \\ 0 & 1 \end{bmatrix} M_i \begin{bmatrix} \sigma_x I_{n_x} & 0 \\ 0 & 1 \end{bmatrix} \right)^{-1}, \end{aligned}$$

with M_i , $i \in [0, n_u]$, defined in (7). If M_i , $i \in [0, n_u]$, has zero as an eigenvalue, we define the inverse of that eigenvalue to be infinity.

PROOF. The result directly follows by using Lemma 7 and (Dean et al., 2020, Proposition 2.4) with $\frac{\delta}{2}$ followed by union bound arguments. \square

With this, we have established a priori and data-dependent finite sample identification error bounds for the identification of bilinear systems from i. i. d. data.

While the results hold for bilinear systems, Koopman operator theory provides an appealing tool to extend the results of this work to more general nonlinear systems. While a detailed analysis is out of the scope of this work, we sketch some of the links between our results and the general nonlinear case in the following.

3.4 Implications for data-driven control of nonlinear systems

As already discussed, Koopman operator theory (Koopman, 1931; Mauroy et al., 2020) allows to accurately represent nonlinear systems by higher-dimensional bilinear systems (Surana, 2016; Huang et al., 2018). Identifying this lifted bilinear system from data collected from the true system is an active field of research. Although (extended) dynamic mode decomposition (Williams et al., 2015) is shown to suitably approximate the Koopman operator (Korda and Mezić, 2018; Bevanda et al., 2021) while being scalable to large-scale systems and robust w.r.t. noise (Bevanda et al., 2024; Meanti et al., 2024), finite sample identification error bounds are usually hard to obtain for noisy systems (Mezić, 2022; Nüske et al., 2023; Philipp et al., 2024). One particular challenge lies in the fact that we cannot sample from the high-dimensional lifted state-space directly, but only from the lower-dimensional original state-space, where the two are related by known lifting functions. Here, we emphasize that sampling in the original state space and lifting the samples afterwards does not violate the assumptions of Theorem 9. Thus, this result can still be applied to a setting where the system is bilinear in a lifted state space. Regarding Theorem 8, the following proposition demonstrates for a particular choice of a lifting function, which has been widely used in the Koopman literature, that sub-Gaussian sampling in the lifted state space (Assumption 2) can still be satisfied, enabling the application of Theorem 8 in this setup.

Lemma 10 Consider a scalar random variable $x \stackrel{i.i.d.}{\sim} U(a)$. Then, the random vector $\xi = [x \sin(x)]^\top$ is sub-Gaussian distributed with variance proxy

$$\sigma^2 \leq \begin{cases} 2a + 1, & \text{if } a \in (0, 1], \\ a^2 + 2a, & \text{if } a \in (1, \infty). \end{cases}$$

PROOF. See Appendix B. \square

Although we provide the proof for a scalar variable x for clarity of exposition, Lemma 10 can be easily extended to vector-valued random variables, where $\sin(\cdot)$ is applied element-wise. While we show that a suitable sampling in the original state space ensures sub-Gaussian sampling in the lifted space for a specific lifting function, this remains an open question for general lifting functions. However, we conjecture that Lemma 10 can be extended to other classes of lifting functions using bounded sampling, where similar results hold for Lipschitz continuous lifting functions (Wainwright, 2019, Theorem 2.26). Further, note that the derived upper bound of the variance proxy is

not sharp, but shows that lifted samples are sub-Gaussian distributed. Finding the exact variance proxy (or a tight lower bound) and a dedicated analysis for commonly used lifting functions are interesting directions for future research.

4 Controller design for bilinear systems

For the controller design, we consider the system representation in (2) but focus on the noise-free part of the dynamics, i.e., our control objective is nominal stabilization. In particular, we assume that the only uncertainty in the system dynamics arises from the identification error, which is a common assumption in nonlinear data-driven control, see, e.g., Martin et al. (2023); Faulwasser et al. (2023) and the references therein. More precisely, we express (2) in terms of the OLS estimates \hat{A} , $\hat{B}_0 = [\hat{B}_0]_1 \cdots [\hat{B}_0]_{n_u}]$, $\hat{B}_1, \dots, \hat{B}_{n_u}$ and define $\hat{A}_{ux} = [\hat{B}_1 - \hat{A} \cdots \hat{B}_{n_u} - \hat{A}]$ to obtain the uncertain bilinear system

$$x_t^+ = \hat{A}x_t + \hat{B}_0u_t + \hat{A}_{ux}(u_t \otimes x_t) + r(x_t, u_t). \quad (27)$$

Here, $r(x, u)$ is the residual capturing the identification error resulting from the OLS estimation and is given by $r(x, u) = (A - \hat{A})x + (B_0 - \hat{B}_0)u + (A_{ux} - \hat{A}_{ux})(u \otimes x)$. (28)

In the following, we demonstrate that the non-asymptotic identification error bounds derived in Section 3 are suitable for robust control of bilinear systems. Therefore, we follow the design proposed in Strässer et al. (2023, 2024) in the context of a Koopman-based bilinear surrogate model. To this end, we express the obtained error bound as a quadratic matrix inequality that bounds the residual in a proportional manner, i.e.,

$$\|r(x, u)\|_2^2 \leq \begin{bmatrix} x \\ u \end{bmatrix}^\top Q_\Delta \begin{bmatrix} x \\ u \end{bmatrix}. \quad (29)$$

Further, we assume that the control inputs u satisfy $u \in \mathbb{U}$, where $\mathbb{U} \subset \mathbb{R}^{n_u}$ is a user-defined compact set. This is motivated by the fact that u is typically bounded in practice, e.g., due to physical constraints.

In Section 4.1 and Section 4.2, we first derive the quadratic error bound (29) for the individual and ellipsoidal identification error bounds, respectively. Then, we present a regional and a global controller design based on the error bounds derived in Section 4.3.

4.1 Individual identification error bounds

In this section, we consider the individual identification error bounds presented in Theorem 8. The following proposition characterizes how the results in Theorem 8 can be transferred to the error bound (29).

Proposition 11 *Consider the bilinear system (2) and let the identification error be bounded according to (23) with probability at least $1 - \delta$ with $\delta \in (0, 1)$. Then, the residual*

$r(x, u)$ *of the uncertain bilinear system (27) satisfies the quadratic bound (29) for*

$$Q_\Delta = \begin{bmatrix} 2c_x^2 I_{n_x} & 0 \\ 0 & 2c_u^2 I_{n_u} \end{bmatrix} \quad (30)$$

with probability at least $1 - \delta$, where

$$c_x = \left[\max_{u \in \mathbb{U}} \left| 1 - \sum_{i=1}^{n_u} [u]_i \right| \right] \varepsilon_A + \left[\max_{u \in \mathbb{U}} \sum_{i=1}^{n_u} |[u]_i| \varepsilon_{B_i} \right], \quad (31a)$$

$$c_u = \sqrt{\sum_{i=1}^{n_u} \varepsilon_{[B_0]_i}^2}. \quad (31b)$$

PROOF. See Appendix C. □

Based on the individual identification error bounds derived in Theorem 8, Proposition 11 yields a quadratic bound on the residual. In particular, the bound is proportional to the state and input, allowing a robust controller design since the error bound vanishes at the equilibrium $(x, u) = (0, 0)$. As shown in Section 4.3, this allows to design a stabilizing controller either in a region of attraction (RoA) around the equilibrium or globally.

4.2 Ellipsoidal identification error bounds

Next, we use the ellipsoidal identification error bounds presented in Theorem 9 and derive a corresponding matrix Q_Δ . Here, we consider a block-wise decomposition

of the matrices $\mathcal{E}_{B_i} = \begin{bmatrix} [\mathcal{E}_{B_i}]_{11} & [\mathcal{E}_{B_i}]_{12} \\ [\mathcal{E}_{B_i}]_{21} & [\mathcal{E}_{B_i}]_{22} \end{bmatrix}$ in (26b), where $[\mathcal{E}_{B_i}]_{11} \in \mathbb{R}^{n_x \times n_x}$, $[\mathcal{E}_{B_i}]_{12} = [\mathcal{E}_{B_i}]_{21}^\top \in \mathbb{R}^{n_x}$, $[\mathcal{E}_{B_i}]_{22} \in \mathbb{R}$.

Proposition 12 *Consider the bilinear system (2) and let the identification error be bounded according to (26) with probability at least $1 - \delta$ with $\delta \in (0, 1)$. Then, the residual $r(x, u)$ of the uncertain bilinear system (27) satisfies the quadratic bound (29) for*

$$Q_\Delta = \begin{bmatrix} (n_u + 1) \max_{u \in \mathbb{U}} \left| 1 - \sum_{i=1}^{n_u} [u]_i \right|^2 \mathcal{E}_A & 0 \\ 0 & 0 \end{bmatrix} + (n_u + 1) \hat{\mathcal{E}}_B \quad (32a)$$

with probability at least $1 - \delta$, where

$$\hat{\mathcal{E}}_B = [\star]^\top \tilde{\mathcal{E}}_B \begin{bmatrix} (\max_{u \in \mathbb{U}} |u| \otimes I_{n_x}) & 0 \\ 0 & I_{n_u} \end{bmatrix}, \quad (32b)$$

$$\tilde{\mathcal{E}}_B = \begin{bmatrix} [\mathcal{E}_{B_1}]_{11} & & [\mathcal{E}_{B_1}]_{12} & \\ & \ddots & & \ddots \\ & & [\mathcal{E}_{B_{n_u}}]_{11} & [\mathcal{E}_{B_{n_u}}]_{12} \\ \hline [\mathcal{E}_{B_1}]_{21} & & [\mathcal{E}_{B_1}]_{22} & \\ & \ddots & & \ddots \\ & & [\mathcal{E}_{B_{n_u}}]_{21} & [\mathcal{E}_{B_{n_u}}]_{22} \end{bmatrix}.$$

PROOF. See Appendix D. \square

Similar to the discussion for the individual identification error bounds, Proposition 12 establishes an error characterization of the residual which is tailored to control and vanishes at the origin.

4.3 Controller design

In the following, we present the proposed controller designs for system (2) based on the identified bilinear system (27). To this end, we propose two different designs for regional and global stability guarantees in Sections 4.3.1 and 4.3.2, respectively, where the former is based on linear robust control techniques, while the latter relies on SOS optimization. Depending on the practical application, the different designs offer a trade-off between control performance, the size of the RoA, and computational complexity.

4.3.1 Regional controller design via linear robust control techniques

First, we rely on the state-feedback controller design presented in Strässer et al. (2023, 2024). Here, the controller design of the uncertain bilinear system (27) is addressed by *linear* robust control techniques, which are based on rewriting the bilinear system as a linear fractional representation (Zhou et al., 1996) within a user-defined state region $\mathcal{X} \subset \mathbb{R}^{n_x}$. To this end, we define the set

$$\mathcal{X} = \left\{ x \in \mathbb{R}^{n_x} \left| \begin{bmatrix} x \\ 1 \end{bmatrix}^\top \begin{bmatrix} Q_x & S_x \\ S_x^\top & R_x \end{bmatrix} \begin{bmatrix} x \\ 1 \end{bmatrix} \geq 0 \right. \right\}, \quad (33)$$

where $Q_x \prec 0$ and $R_x > 0$. Then, the proposed controller design guarantees invariance of \mathcal{X} and regional stability of the closed loop for initial conditions in a subset of \mathcal{X} . Possible choices are, e.g., $Q_x = -I$, $S_x = 0$, and $R_x = c$ defining a norm bound on the state $\|x\|^2 \leq c$. An algorithm to heuristically optimize the geometry of \mathcal{X} based on the identified system dynamics is given in (Strässer et al., 2025d, Procedure 8), to which we also refer for a discussion on how the resulting control behavior is affected by the choice of \mathcal{X} . Further, we assume $u(x) \in \mathbb{U}$ for all $x \in \mathcal{X}$ and existence of $\begin{bmatrix} \tilde{Q}_x & \tilde{S}_x \\ \tilde{S}_x^\top & \tilde{R}_x \end{bmatrix} := \begin{bmatrix} Q_x & S_x \\ S_x^\top & R_x \end{bmatrix}^{-1}$.

Theorem 13 Consider the bilinear system (2), where the residual of the system identification satisfies (29) for some Q_Δ with probability at least $1 - \delta$ with $\delta \in (0, 1)$. If there exist $P = P^\top \succ 0$ of size $n_x \times n_x$, $L \in \mathbb{R}^{n_u \times n_x}$, $L_w \in \mathbb{R}^{n_u \times n_x n_u}$, $\Lambda = \Lambda^\top \succ 0$ of size $n_u \times n_u$, and $\nu > 0$, $\tau > 0$ such that the LMIs (34) and

$$\begin{bmatrix} \nu \tilde{R}_x - 1 & -\nu \tilde{S}_x^\top \\ -\nu \tilde{S}_x & \nu \tilde{Q}_x + P \end{bmatrix} \preceq 0 \quad (35)$$

hold, then the controller

$$u = \kappa_{\text{reg}}(x) = (I - L_w(\Lambda^{-1} \otimes x))^{-1} L P^{-1} x \quad (36)$$

ensures exponential stability of the closed-loop system for all initial conditions in $\mathcal{X}_{\text{RoA}} := \{x \in \mathbb{R}^{n_x} \mid x^\top P^{-1} x \leq 1\} \subseteq \mathcal{X}$ with probability at least $1 - \delta$.

PROOF. This is a direct combination of (Strässer et al., 2023, Theorem 4) and (Strässer et al., 2024, Theorem 4.1), where we generalize the result by exploiting Q_Δ in (29) for the error bound on the residual. \square

Theorem 13 establishes a controller design for the unknown bilinear system (2) with end-to-end guarantees based on measured data. In particular, the controller design ensures exponential stability of the closed-loop system for all initial conditions in the RoA \mathcal{X}_{RoA} with high probability. To this end, we exploit the identified system dynamics and the identification error bounds derived in Section 3 to establish a controller design that is robust to the residual. Here, we can use the individual or the ellipsoidal identification error bounds to derive the matrix Q_Δ used in the controller design, see (30) and (32), respectively. The design scheme requires and ensures that the state x remains within the set \mathcal{X} . Thus, the set \mathcal{X} needs to be carefully chosen when applying the controller design. More precisely, if the controller design is not feasible for a given set of data, feasibility might be ensured by either collecting more data to reduce the identification error or adjusting the set \mathcal{X} to shrink the guaranteed RoA $\mathcal{X}_{\text{RoA}} \subseteq \mathcal{X}$. Thus, the controller design can be iterated until successful, see Algorithm 2. Note that the controller design is cast as a semi-definite program (SDP), which can be efficiently solved. We observe that the computational complexity of the LMIs (34), (35) is $\mathcal{O}((3n_x + n_u(2 + n_x))^6)$. This can be challenging for large-scale systems and, hence, future work should investigate structure-exploiting SDP techniques (De Klerk, 2010; Gramlich et al., 2023).

4.3.2 Global controller design via SOS optimization

Next, we propose a global controller design based on SOS optimization techniques¹. The main motivation for this is that choosing the pre-defined set \mathcal{X} may be restrictive for some applications. Instead, we aim to design a rational controller that ensures global stability of the closed-loop system with high probability for all initial conditions. To this end, we generalize the SOS optimization-based controller design proposed in Strässer et al. (2025a) to handle the identification error bound (29) with matrix Q_Δ .

Theorem 14 Consider the bilinear system (2), where the residual of the system identification satisfies (29) for some Q_Δ with probability at least $1 - \delta$ with $\delta \in (0, 1)$. If there exist $\alpha > 0$, $P = P^\top \succ 0$ of size $n_x \times n_x$, $L_n \in \mathbb{R}[x, 2\alpha -$

¹ We define $\mathbb{R}[x, d]$ as the set of all polynomials s in the variable $x \in \mathbb{R}^n$ with real coefficients and degree at most d , i.e., $s(x) = \sum_{\alpha \in \mathbb{N}_0^n, |\alpha| \leq d} s_\alpha x^\alpha$, where $s_\alpha \in \mathbb{R}$ and $|\alpha| \leq d \in \mathbb{N}_0$. Here, the monomials are given by $x^\alpha = x_1^{\alpha_1} \cdots x_n^{\alpha_n}$ for a multi-index $\alpha \in \mathbb{N}_0^n$ with $|\alpha| = \alpha_1 + \cdots + \alpha_n$. The set of all $p \times q$ -matrices whose elements belong to $\mathbb{R}[x, d]$ is denoted by $\mathbb{R}[x, d]^{p \times q}$. A matrix $S \in \mathbb{R}[x, 2d]^{p \times p}$ is called SOS matrix in x if it can be decomposed as $S = T^\top T$ for some $T \in \mathbb{R}[x, d]^{q \times p}$, where we write $S \in \text{SOS}[x, 2d]^p$. Finally, $S \in \mathbb{R}[x, 2d]^{p \times p}$ is said to be strictly SOS if there exists $\varepsilon > 0$ such that $(S - \varepsilon I_p) \in \text{SOS}[x, 2d]^p$, denoted by $S \in \text{SOS}_+[x, 2d]^p$.

$$\begin{bmatrix}
P - \tau I_{n_x} & -\hat{A}_{ux}(\Lambda \otimes \tilde{S}_x) - \hat{B}_0 L_w (I_{n_u} \otimes \tilde{S}_x) & 0 & \hat{A}P + \hat{B}_0 L & \hat{A}_{ux}(\Lambda \otimes I_{n_x}) + \hat{B}_0 L_w \\
\star & \Lambda \otimes \tilde{R}_x - L_w (I_{n_u} \otimes \tilde{S}_x) - (I_{n_u} \otimes \tilde{S}_x^\top) L_w^\top & -(I_{n_x} \otimes \tilde{S}_x^\top) & \begin{bmatrix} 0 \\ L_w \end{bmatrix} & L & L_w \\
\star & \star & \tau Q_\Delta^{-1} & \begin{bmatrix} P \\ L \end{bmatrix} & -\begin{bmatrix} 0 \\ L_w \end{bmatrix} \\
\star & \star & \star & P & 0 \\
\star & \star & \star & \star & -\Lambda \otimes \tilde{Q}_x^{-1}
\end{bmatrix} \succ 0 \quad (34)$$

Algorithm 2 Indirect DDC with end-to-end guarantees

- 1: Choose $\delta, T_0, \dots, T_{n_u}$
- 2: Collect data and identify system matrices using Algorithm 1 with the sampling scheme chosen according to the desired error bounds
- 3: Attempt controller design:
 - a) *Regional controller design (Theorem 13)*
- 4a: Choose \mathcal{X} in (33)
- 5a: **if** LMIs (34) and (35) are feasible **then**
- 6a: Controller (36) yields closed-loop exponential stability in $\mathcal{X}_{\text{RoA}} \subseteq \mathcal{X}$ with high probability
- 7a: **else**
- 8a: Modify parameters in 1 until successful
- 9a: **end if**
- b) *Global controller design (Theorem 14)*
- 4b: **if** SOS condition (37) is feasible **then**
- 5b: Controller κ_{glob} yields global closed-loop exponential stability with high probability
- 6b: **else**
- 7b: Modify parameters in 1 until successful
- 8b: **end if**

$1]^{n_u \times n_x}, \tau \in \text{SOS}_+[x, 2\alpha], u_d \in \text{SOS}_+[x, 2\alpha], \text{ and } \rho > 0$ such that

$$\begin{bmatrix}
u_d P - \tau I_{n_x} - \rho u_d I_{n_x} & \star & \star \\
0 & \tau Q_\Delta^{-1} & \star \\
(u_d \hat{A}P + \hat{B}_0 L_n + \hat{A}_{ux}(L_n \otimes x))^\top \begin{bmatrix} u_d P \\ L_n \end{bmatrix}^\top & u_d P
\end{bmatrix} \quad (37)$$

is in $\text{SOS}[x, 2\alpha]^{3n_x + n_u}$, then the controller

$$u = \kappa_{\text{glob}}(x) = \frac{1}{u_d(x)} L_n(x) P^{-1} x \quad (38)$$

ensures global exponential stability of the closed-loop bilinear system with probability at least $1 - \delta$.

PROOF. This is a direct consequence of (Strässer et al., 2025a, Theorem 2), generalized by using Q_Δ in (29) for the error bound on the residual. \square

Theorem 14 establishes a controller design for the unknown bilinear system (2) with global end-to-end guarantees based on measured data. In particular, the controller design ensures *global* exponential stability of the closed-loop system with high probability. Note that the SOS program (37) is linear in the decision variables P, L_n, τ, ρ for a fixed polynomial u_d , and can be solved using convex

optimization techniques (Papachristodoulou and Prajna, 2005). Here, the a priori chosen u_d acts as a tuning parameter, providing an additional degree of freedom in the controller parametrization. Compared to Theorem 13, the SOS-based design in Theorem 14 does not rely on a predefined state region \mathcal{X} and, hence, is applicable to a wider range of systems. On the other hand, the SOS optimization with complexity $\mathcal{O}((3n_x + n_u)^6 n_x^{6\alpha})$ is computationally more demanding and, hence, might not be suitable for large-scale systems. Moreover, a higher degree α in the controller design allows for a more flexible controller design, but it also increases the computational complexity of the SOS program. Thus, both controller designs offer a trade-off between control performance, the size of the RoA, and computational complexity.

For the controller design, we assume that the system is not affected by noise, which is a common assumption in the literature on (stochastic) data-driven control (Martin et al., 2023; Faulwasser et al., 2023). However, since the SOS-based controller *globally* exponentially stabilizes the nominal bilinear system, (Culbertson et al., 2023, Corollary 2) implies exponential input-to-state stability (ISS) in probability. Thus, the trajectories of the perturbed closed loop remain bounded with high probability when the process noise is present during operation (Culbertson et al., 2023, Corollary 3). Culbertson et al. (2023) also note that the choice of the Lyapunov function is crucial to reduce conservatism of the ISS guarantees. To this end, it may be beneficial to incorporate the noise directly in the controller design via an additional uncertainty channel, and we defer this controller design improvement to future research.

5 Numerical examples

In this section, we first provide numerical simulations to illustrate the derived identification error bounds of Section 3 (Section 5.1), where we compare the a priori identification error bounds (Theorem 5) with the data-dependent bounds (Theorem 6). Second, we use both types of the identification error bounds to design a controller for a bilinear system providing end-to-end guarantees for indirect data-driven control (Section 5.2).²

² The code for the numerical examples can be accessed at: <https://github.com/col-tasas/2024-bilinear-end-to-end>

5.1 Error bounds

In this section, we analyze the identification error bounds derived in Section 3 with respect to conservatism and dependence on key problem parameters. Here, we focus our analysis on the identification problem (3b) and refer to the works by Dean et al. (2020) or Matni and Tu (2019) for the analysis of the identification error bounds of (3a). For the remainder of this section the setup will be as follows. Data is collected by sampling $x_k \stackrel{\text{i.i.d.}}{\sim} \mathcal{N}(0, I)$ and evaluating the unknown, affine function

$$x_t^+ = B_1 x_t + B_0 + w_t,$$

where $w_t \stackrel{\text{i.i.d.}}{\sim} \mathcal{N}(0, \sigma_w^2 I_{n_x})$, $\sigma_w = 0.5$. The matrix $B_1 \in \mathbb{R}^{n_x \times n_x}$ and the vector $B_0 \in \mathbb{R}^{n_x}$ are drawn randomly. We estimate B_1 and B_0 using the OLS estimate (6b).

First, we consider the influence of the sample size on the identification error. To this end, we select $n_x = 25$. Further, we empirically estimate the identification error through Monte Carlo simulations to average out the randomness in the noise and data-sampling. Since the data-dependent identification error bound (25b) also depends on the observed data, we consider the mean over the Monte Carlo simulations. The mean and 3σ -band of the empirically approximated identification error as well as the mean of the data-based bound are displayed in Fig. 1(a) along with the a priori sample complexity bounds. The results show that the a priori identification error bounds are more conservative than their data-dependent counterparts. This is to be expected since the data-dependent identification error bounds only take into account the data that is observed and need less potentially conservative steps in their derivation. Further, even in a high-data regime, both bounds overestimate the true identification error, where as expected the absolute value of the gap decreases as the number of samples increases. Additionally, Fig. 1(b) shows that the dependency $\mathcal{O}(1/\sqrt{T})$ on the sample size captured in the a priori identification error bound is correct.

Now, we focus on the dependence on the problem dimension n_x . To this end, we consider random B_1 and B_0 with n_x varying between 1 and 30. Again, we use Monte Carlo simulations to evaluate the identification errors and identification error bounds for $T = 250\,000$ samples. The results are displayed in Fig. 1(c). It is apparent that the identification error increases as expected with the problem size. However, as shown in Fig. 1(d), the conservatism of the error bounds decreases as the problem size n_x increases. As before, the data-based bound is consistently less conservative than the a priori bound.

5.2 Controller design

Next, we study the incorporation of the different types of identification error bounds in control. In particular, we design a controller for the bilinear system (2) following Theorems 13 and 14 with both the individual identification error bounds of Section 4.1 as well as the ellipsoidal identification error bounds of Section 4.2. Here, we study

Table 1

Required data length for a feasible controller design for the academic example in Section 5.2.1.

	$\kappa_{\text{reg}}(x_t)$, RoA: $\ x_t\ _2^2 \leq c$	$\kappa_{\text{glob}}(x_t)$		
	$c = 0.1$	$c = 0.6$	$c = 0.9$	$x_t \in \mathbb{R}^2$
Indiv.	$T = 360$	$T = 2263$	$T = 34\,668$	$T = 5145$
Ellips.	$T = 33$	$T = 213$	$T = 3999$	$T = 959$
Comp. time	0.0055 s	0.0066 s	0.0070 s	0.0135 s

the different error bounds in terms of 1) the feasibility of the controller designs depending on the data length, and 2) the size of the guaranteed RoA of the regional design in Theorem 13. We note that we do not consider the a priori identification error bounds in the controller design, as they are more conservative than the data-dependent bounds according to the previous section. The simulations are performed in MATLAB using the YALMIP toolbox (Löfberg, 2004) with its SOS modul (Löfberg, 2009) and the solver MOSEK (MOSEK, 2022).

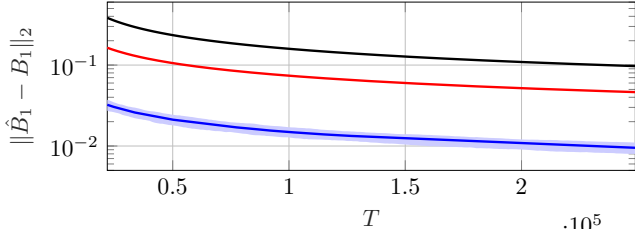
5.2.1 Academic example

We start by considering the dynamical system

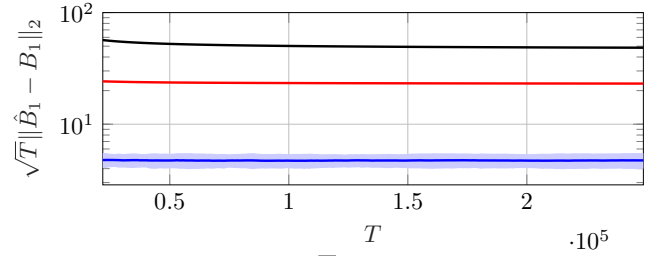
$$x_t^+ = \begin{bmatrix} 1 & 1 \\ 0 & 1 \end{bmatrix} x_t + \begin{bmatrix} 1 \\ 1 \end{bmatrix} u_t + \begin{bmatrix} 1 & 0 \\ 0 & 1 \end{bmatrix} u_t x_t + w_t, \quad (39)$$

where we assume a compact input space $\mathbb{U} = [-2, 2]$. For the *regional* controller design in Section 4.3.1, we define the region of interest \mathcal{X} in (33) via the norm bound $\|x_t\|_2^2 \leq c$. We emphasize once again that with high probability the RoA $\mathcal{X}_{\text{RoA}} \subseteq \mathcal{X}$ is invariant under our control law (36), where \mathcal{X}_{RoA} corresponds to the sublevel set $V(x) \leq 1$ of the Lyapunov function $V(x) = x^\top P^{-1} x$ with $P \succ 0$. Hence, we maximize the trace of P subject to the LMIs (34), (35) to find the largest RoA. On the other hand, the controller design in Section 4.3.2 yields a *globally* stabilizing controller, where we choose $\alpha = 1$ and $u_d(x) = 1 + [x_t]_1^2 + [x_t]_1 [x_t]_2 + [x_t]_2^2$.

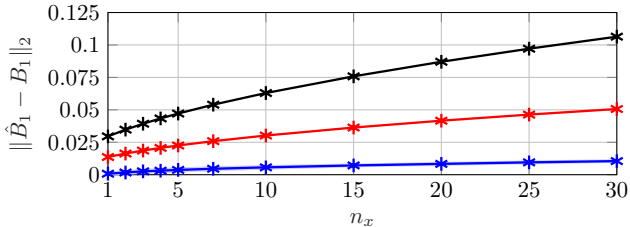
First, we study the feasibility of the controller designs for the two types of identification error bounds. In particular, we select $w_t \stackrel{\text{i.i.d.}}{\sim} \mathcal{N}(0, \sigma_w^2 I)$ with $\sigma_w = 0.1$, $\delta = 0.05$, sample $x_t \stackrel{\text{i.i.d.}}{\sim} \mathcal{N}(0, I)$, and numerically determine the minimally required data lengths. Here, we restrict ourselves to data lengths $T_0 = T_1 = T$, but note that generally the lengths could be chosen differently. The results in Table 1 show that the ellipsoidal error bounds require less data to design a feasible controller compared to the individual error bounds. In other words, the ellipsoidal error bounds allow for larger RoA for a given data length. This is in line with Fig. 2, where we show the RoAs corresponding to the simulations in Table 1. We emphasize that the RoA of the regional controller design is determined by P whose trace is maximized in the controller design and, thus, the obtained RoA for more data is not necessarily a superset



(a) Error for different sample sizes.

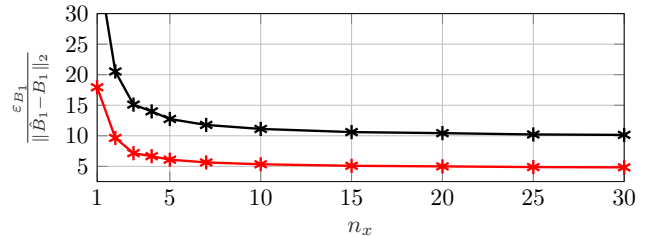


(b) Error times \sqrt{T} over sample size.



(c) Error for different problem dimensions.

Fig. 1. Mean of the identification error (—), data-based bounds (—), and a priori error bounds (—) through 100 Monte Carlo simulations. Shaded areas are respective 3σ -bands.



(d) Error bounds relative to mean Monte Carlo error.

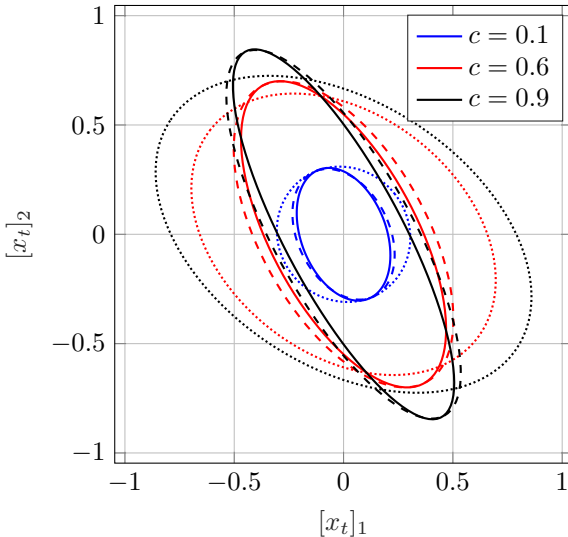


Fig. 2. RoA of the academic example for $\mathcal{X} = \{x \mid \|x\|^2 \leq c\}$ and the minimum required data length for individual error bounds (—) and ellipsoidal error bounds (---) as well as the RoA with ellipsoidal error bounds for the minimum data length required for individual error bounds (.....).

of the RoA for less data. However, this could be ensured by adding a suitable set-containment constraint to the optimization problem, which would come at the cost of less degrees of freedom in the controller design. Notably, the SOS controller κ_{glob} is globally stabilizing, i.e., on the entire state space \mathbb{R}^2 , and it is feasible for less data than the regional controller for $\|x_t\|_2^2 \leq 0.9$. However, the complexity of the SOS controller design is higher than the regional controller design, which is reflected in the computation times in Table 1.

5.2.2 Nonlinear inverted pendulum

Next, we illustrate the application of our results to a nonlinear system using the link with Koopman operator theory discussed in Section 3.4. To this end, we consider the nonlinear inverted pendulum (Tiwari et al., 2023; Verhoek et al., 2023; Strässer et al., 2025d)

$$z_t^+ = \begin{bmatrix} [z_t]_1 + T_s [z_t]_2 \\ [z_t]_2 + \frac{T_s g}{l} \sin([z_t]_1) - \frac{T_s b}{ml^2} [z_t]_2 + \frac{T_s}{ml^2} u_t \end{bmatrix} \quad (40)$$

with mass $m = 1 \text{ kg}$, length $l = 1 \text{ m}$, damping coefficient $b = 0.5$, gravitational acceleration $g = 9.81 \text{ m/s}^2$ and $T_s = 0.1 \text{ s}$. We follow Section 3.4 and define the lifting function $x = \Phi(z) = [[z]_1 \ [z]_2 \ \sin([z]_1)]^\top$ leading to an uncertain bilinear system representation in x . Here, we assume that the lifting function Φ gives an exact finite-dimensional Koopman representation of the system dynamics. However, we emphasize that, when an exact lifting is unknown, the approximation error of the (finite-dimensional) Koopman representation cannot be neglected in the controller design, see Strässer et al. (2025b,c) for a detailed discussion. For the simulation, we select $w_t \stackrel{\text{i.i.d.}}{\sim} \mathcal{N}(0, \sigma_w^2 I)$ with $\sigma_w = 0.001$, $\delta = 0.05$, sample $z_t \stackrel{\text{i.i.d.}}{\sim} \mathcal{N}(0, I)$. Then, we assume a compact input space $\mathbb{U} = [-2, 2]$ and collect $T_0 = T_1 = 50\,000$ data samples. Following Theorem 9 and Algorithm 2, we determine the corresponding ellipsoidal error bounds and the respective Q_Δ in (32). For the SOS-based controller design in Theorem 14, we observe that feasibility improves when over-estimating the error bound by choosing $\tilde{Q}_\Delta = \|Q_\Delta\|_2 I$ in the quadratic expression in (29). Clearly, if the controller is robust w.r.t. the over-estimated error bound, then it is also robust w.r.t. the actual error bound. The obtained closed-loop trajectories

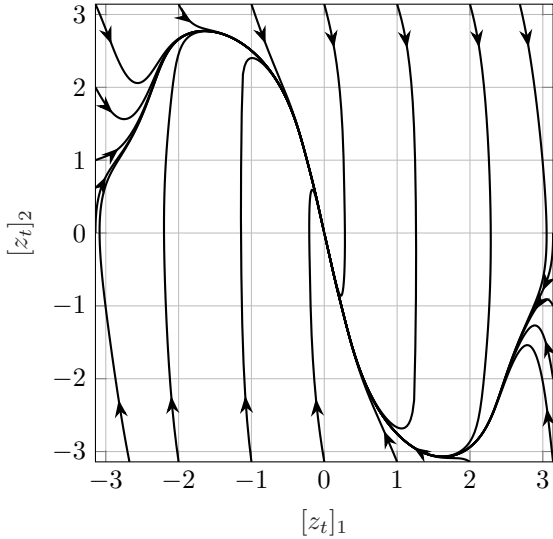


Fig. 3. Closed-loop trajectories of the nonlinear inverted pendulum example in Section 5.2.2 with the SOS controller $\kappa_{\text{glob.}}$.

are depicted in Fig. 3 to illustrate the controller's performance. Overall, these results show that our approach can be applied to nonlinear systems using the link with Koopman operator theory, paving the way towards the design of data-driven controllers for nonlinear systems using data affected by stochastic noise.

6 Conclusion

In this work, we leveraged tools from statistical learning theory to derive finite sample identification error bounds for the identification of unknown bilinear systems from noisy data. The derived identification error bounds are then combined with robust control for bilinear systems to obtain an exponentially stable closed loop. The presented numerical studies show the interplay between identification error bounds and controller design. To the best of our knowledge, this is the first work connecting statistical learning theory results with robust control to provide end-to-end guarantees for indirect data-driven control of bilinear systems from finite data affected by potentially unbounded stochastic noise. We note that the results of this work provide a promising avenue for indirect data-driven control of nonlinear systems by means of Koopman operator theory and view this as an interesting direction for future work.

References

Abbasi-Yadkori, Y., Pál, D., Szepesvári, C., 2011. Improved algorithms for linear stochastic bandits. In: Advances in Neural Information Processing Systems. Vol. 24.

Amato, F., Cosentino, C., Fiorillo, A. S., Merola, A., 2009. Stabilization of bilinear systems via linear state-feedback control. *IEEE Trans. on Circuits and Systems II: Express Briefs* 56 (1), 76–80.

Benallou, A., Mellichamp, D. A., Seborg, D. E., 1988. Optimal stabilizing controllers for bilinear systems. *Int. J. of Control* 48 (4), 1487–1501.

Berk Hizir, N., Phan, M. Q., Betti, R., Longman, R. W., 2012. Identification of discrete-time bilinear systems through equivalent linear models. *Nonlinear Dynamics* 69 (4), 2065–2078.

Bevanda, P., Driessens, B., Iacob, L. C., Tóth, R., Sosnowski, S., Hirche, S., 2024. Nonparametric control-Koopman operator learning: Flexible and scalable models for prediction and control. *arXiv:2405.07312*.

Bevanda, P., Sosnowski, S., Hirche, S., 2021. Koopman operator dynamical models: Learning, analysis and control. *Annual Reviews in Control* 52, 197–212.

Coutinho, D., de Souza, C. E., da Silva, J. M. G., Caldeira, A. F., Prieur, C., 2019. Regional stabilization of input-delayed uncertain nonlinear polynomial systems. *IEEE Trans. Autom. Control* 65 (5), 2300–2307.

Culbertson, P., Cosner, R. K., Tucker, M., Ames, A. D., 2023. Input-to-state stability in probability. In: Proc. 62nd IEEE Conf. on Decision and Control (CDC). pp. 5796–5803.

Dasgupta, S., Shrivastava, Y., Krenzer, G., 1989. Persistent excitation in bilinear systems. In: Proc. 28th IEEE Conf. on Decision and Control (CDC). pp. 1956–1961 vol.3.

De Klerk, E., 2010. Exploiting special structure in semidefinite programming: A survey of theory and applications. *European Journal of Operational Research* 201 (1), 1–10.

Dean, S., Mania, H., Matni, N., Recht, B., Tu, S., 2020. On the sample complexity of the linear quadratic regulator. *Found. of Computational Mathematics* 20 (4), 633–679.

Derese, I., Noldus, E., 1980. Design of linear feedback laws for bilinear systems. *Int. J. of Control* 31 (2), 219–237.

Faulwasser, T., Ou, R., Pan, G., Schmitz, P., Worthmann, K., 2023. Behavioral theory for stochastic systems? a data-driven journey from Willems to Wiener and back again. *Annual Reviews in Control* 55, 92–117.

Favoreel, W., De Moor, B., Van Overschee, P., 1999. Subspace identification of bilinear systems subject to white inputs. *IEEE Trans. Autom. Control* 44 (6), 1157–1165.

Fnaiech, F., Ljung, L., Feb. 1987. Recursive identification of bilinear systems. *Int. J. of Control* 45 (2), 453–470.

Foster, D., Sarkar, T., Raklin, A., 2020. Learning nonlinear dynamical systems from a single trajectory. In: Proc. 2nd Conf. on Learning for Dynamics and Control. PMLR.

Golub, G. H., Van Loan, C. F., 2013. Matrix computations. JHU press.

Gramlich, D., Holicki, T., Scherer, C. W., Ebenbauer, C., 2023. A structure exploiting sdp solver for robust controller synthesis. *IEEE Control Systems Letters* 7, 1831–1836.

Gutman, P.-O., 1980. Controllers for Bilinear Systems. Technical Reports TFRT-7210. Department of Automatic Control, Lund Institute of Technology (LTH).

Gutman, P.-O., 1981. Stabilizing controllers for bilinear systems. *IEEE Trans. Autom. Control* 26 (4), 917–922.

Huang, B., Ma, X., Vaidya, U., 2018. Feedback stabilization using Koopman operator. In: Proc. 57th IEEE Conf. on Decision and Control (CDC). pp. 6434–6439.

Huang, Y., Jadbabaie, A., 1999. Nonlinear H_∞ control: An enhanced quasi-LPV approach. *IFAC Proceedings Volumes* 32 (2), 2754–2759.

Khlebnikov, M. V., 2018. Quadratic stabilization of discrete-time bilinear systems. *Automation and Remote Control* 79, 1222–1239.

Koopman, B. O., 1931. Hamiltonian systems and transformation in Hilbert space. *Proc. of the National Academy of Sciences of the United States of America* 17 (5), 315.

Korda, M., Mezić, I., 2018. On convergence of extended dy-

namic mode decomposition to the Koopman operator. *J. of Nonlinear Science* 28 (2), 687–710.

Lin, W., Byrnes, C. I., 1994. KYP lemma, state feedback and dynamic output feedback in discrete-time bilinear systems. *Systems & Control Letters* 23 (2), 127–136.

Ljung, L., 1998. System identification. In: *Signal analysis and prediction*. Springer, pp. 163–173.

Löfberg, J., 2004. YALMIP: A toolbox for modeling and optimization in MATLAB. In: *Proc. IEEE Int. Conf. on Robotics and Automation*. pp. 284–289.

Löfberg, J., 2009. Pre- and post-processing sum-of-squares programs in practice. *IEEE Transactions on Automatic Control* 54 (5), 1007–1011.

Longchamp, R., 1980. Stable feedback control of bilinear systems. *IEEE Trans. Autom. Control* 25 (2), 302–306.

Luesink, R., Nijmeijer, H., 1989. On the stabilization of bilinear systems via constant feedback. *Linear algebra and its applications* 122, 457–474.

Mania, H., Tu, S., Recht, B., 2019. Certainty equivalence is efficient for linear quadratic control. *Advances in Neural Information Processing Systems* 32.

Martin, T., Schön, T. B., Allgöwer, F., 2023. Guarantees for data-driven control of nonlinear systems using semidefinite programming: A survey. *Annual Reviews in Control*, 100911.

Matni, N., Tu, S., 2019. A tutorial on concentration bounds for system identification. In: *Proc. 58th IEEE Conf. on Decision and Control (CDC)*. pp. 3741–3749.

Mauroy, A., Mezić, I., Susuki, Y., 2020. The Koopman operator in systems and control. Springer.

Meanti, G., Chatalic, A., Kostic, V., Novelli, P., Pontil, M., Rosasco, L., 2024. Estimating Koopman operators with sketching to provably learn large scale dynamical systems. *Advances in Neural Information Processing Systems* 36.

Mezić, I., 2022. On numerical approximations of the Koopman operator. *Mathematics* 10 (7), 1180.

Mohler, R. R., 1973. Bilinear control processes: with applications to engineering, ecology and medicine. Academic Press, Inc.

Mohler, R. R., Kolodziej, W., et al., 1980. An overview of bilinear system theory and applications. *IEEE Trans. on Systems, Man and Cybernetics* 10 (10), 683–688.

MOSEK, A., 2022. The MOSEK optimization toolbox for MATLAB manual. Version 9.3.21.

Nüske, F., Peitz, S., Philipp, F., Schaller, M., Worthmann, K., 2023. Finite-data error bounds for Koopman-based prediction and control. *J. of Nonlinear Science* 33 (1), 14.

Papachristodoulou, A., Prajna, S., 2005. A tutorial on sum of squares techniques for systems analysis. In: *Proc. American Control Conference (ACC)*.

Pedrycz, W., 1980. Stabilization of bilinear systems by a linear feedback control. *Kybernetika* 16 (1), 48–53.

Philipp, F. M., Schaller, M., Boshoff, S., Peitz, S., Nüske, F., Worthmann, K., 2024. Variance representations and convergence rates for data-driven approximations of Koopman operators. *arXiv:2402.02494*.

Sarkar, T., Rakhlin, A., 2019. Near optimal finite time identification of arbitrary linear dynamical systems. In: *Int. Conf. on Machine Learning*. PMLR.

Sattar, Y., Jedra, Y., Fazel, M., Dean, S., 2025. Finite sample identification of partially observed bilinear dynamical systems. *arXiv:2501.07652*.

Sattar, Y., Oymak, S., 2022. Non-asymptotic and accurate learning of nonlinear dynamical systems. *J. of Machine Learning Research* 23 (140), 1–49.

Sattar, Y., Oymak, S., Ozay, N., 2022. Finite sample identification of bilinear dynamical systems. In: *Proc. 61st IEEE Conf. on Decision and Control (CDC)*. pp. 6705–6711.

Shirani Faradonbeh, M. K., Tewari, A., Michailidis, G., 2018. Finite time identification in unstable linear systems. *Automatica* 96, 342–353.

Simchowitz, M., Mania, H., Tu, S., Jordan, M. I., Recht, B., 2018. Learning without mixing: Towards a sharp analysis of linear system identification. In: *Conf. On Learning Theory*. PMLR, pp. 439–473.

Sontag, E. D., Wang, Y., Megretski, A., 2009. Input classes for identifiability of bilinear systems. *IEEE Trans. Autom. Control* 54 (2), 195–207.

Strässer, R., Berberich, J., Allgöwer, F., 2025a. Koopman-based control using sum-of-squares optimization: Improved stability guarantees and data efficiency. *Proc. European Control Conference (ECC)*, Preprint: *arXiv:2411.03875*.

Strässer, R., Berberich, J., Allgöwer, F., 2023. Control of bilinear systems using gain-scheduling: Stability and performance guarantees. In: *Proc. 62nd IEEE Conf. on Decision and Control (CDC)*. pp. 4674–4681.

Strässer, R., Berberich, J., Schaller, M., Worthmann, K., Allgöwer, F., 2025b. Koopman-based control of nonlinear systems with closed-loop guarantees. *arXiv:2411.10359*.

Strässer, R., Schaller, M., Berberich, J., Worthmann, K., Allgöwer, F., 2025c. Kernel-based error bounds of bilinear Koopman surrogate models for nonlinear data-driven control. *arXiv:2503.13407*.

Strässer, R., Schaller, M., Worthmann, K., Berberich, J., Allgöwer, F., 2025d. Koopman-based feedback design with stability guarantees. *IEEE Trans. Autom. Control* 70 (1), 355–370.

Strässer, R., Schaller, M., Worthmann, K., Berberich, J., Allgöwer, F., 2024. SafEDMD: A certified learning architecture tailored to data-driven control of nonlinear dynamical systems. *arXiv:2402.03145*.

Surana, A., 2016. Koopman operator based observer synthesis for control-affine nonlinear systems. In: *Proc. 55th IEEE Conf. Decis. Control (CDC)*. pp. 6492–6499.

Tiwari, M., Nehma, G., Lusch, B., 2023. Computationally efficient data-driven discovery and linear representation of nonlinear systems for control. *IEEE Control Systems Letters* 7, 3373–3378.

Tsiamis, A., Ziannikas, I., Matni, N., Pappas, G. J., 2023. Statistical learning theory for control: A finite-sample perspective. *IEEE Control Systems* 43 (6), 67–97.

Tsiamis, A., Ziannikas, I. M., Morari, M., Matni, N., Pappas, G. J., 2022. Learning to control linear systems can be hard. In: *Proc. 35th Conf. on Learning Theory*. PMLR.

Underwood, C. P., 2002. HVAC control systems: Modelling, analysis and design. Routledge.

Verhoek, C., Abbas, H. S., Tóth, R., 2023. Direct data-driven LPV control of nonlinear systems: An experimental result. *IFAC-PapersOnLine* 56 (2), 2263–2268.

Vershynin, R., 2012. *Introduction to the non-asymptotic analysis of random matrices*. Cambridge Univ. Press, pp. 210–268.

Wainwright, M. J., 2019. *High-dimensional statistics: A non-asymptotic viewpoint*. Vol. 48. Cambridge Univ. Press.

Williams, M., Kevrekidis, I., Rowley, C., 08 2015. A data-driven approximation of the Koopman operator: Extending dynamic mode decomposition. *J. of Nonlinear Science*

25 (6), 1307–1346.
 Zhou, K., Doyle, J. C., Glover, K., et al., 1996. Robust and optimal control. Vol. 40. Prentice Hall New Jersey.
 Ziemann, I., Tsiamis, A., Lee, B., Jedra, Y., Matni, N., Papas, G. J., 2023. A tutorial on the non-asymptotic theory of system identification. In: Proc. 62nd IEEE Conf. on Decision and Control (CDC). pp. 8921–8939.

A Technical results for the proof of Theorem 5

In the following, we provide technical results used throughout the proof of Theorems 4 and 5. The following proposition is a generalization of (Matni and Tu, 2019, Prop III.1) to sub-Gaussian noise and sampling.

Proposition 15 *Let $x_t \stackrel{i.i.d.}{\sim} \text{subG}_{n_x}(\sigma_x^2)$ and $w_t \stackrel{i.i.d.}{\sim} \text{subG}_{n_x}(\sigma_w^2)$. Fix a failure probability $\delta \in (0, 1)$ and let $T_i \geq \frac{1}{2} \log(9^{2n_x}/\delta)$, then it holds that*

$$\mathbb{P} \left[\left\| \sum_{t=1}^{T_i} x_t w_t^\top \right\|_2 \leq 4\sigma_x \sigma_w \sqrt{T_i \log(9^{2n_x}/\delta)} \right] \leq 1 - \delta.$$

PROOF. The proof can be carried out in the same way as the proof of (Matni and Tu, 2019, Prop. III.1). \square

The following Proposition provides a lower bound on the smallest eigenvalue of a covariance-like matrix and is a variant of (Vershynin, 2012, Theorem 5.39).

Proposition 16 *Let $x_t \stackrel{i.i.d.}{\sim} \text{subG}_{n_x}(\sigma_x^2)$. Fix a failure probability $\delta \in (0, 1)$ and some $c \in (0, \frac{1}{2})$. Let $T_i \geq \frac{8}{c^2} \log(2 \cdot 9^{n_x}/\delta)$. Then it holds that*

$$\mathbb{P} \left[\lambda_{\min} \left(\sum_{t=1}^{T_i} x_t x_t^\top \right) \geq \sigma_x T_i (1 - 2c)^2 \right] \geq 1 - \delta.$$

PROOF. First we define $\sigma_x y_t = x_t$, such that $y_t \stackrel{i.i.d.}{\sim} \text{subG}_{n_x}(1)$. Now note that $\sum_{t=1}^{T_i} x_t x_t^\top = \sigma_x^2 \sum_{t=1}^{T_i} y_t y_t^\top$, i.e., it suffices to analyze the smallest eigenvalue of $Z = \sum_{t=1}^{T_i} y_t y_t^\top$. Next, observe that $Z = Y^\top Y$, with $Y = [y_1 \ y_2 \ \cdots \ y_{T_i}]^\top$ and using this definition it holds that $\sigma_{\min}^2(Y) = \lambda_{\min}(Z)$, where $\sigma_{\min}(Y)$ denotes the smallest singular value of Y . Applying (Vershynin, 2012, Lemma 5.36) with $B = \frac{1}{\sqrt{T_i}} Y$ yields

$$\left\| \frac{1}{T_i} Y^\top Y - I \right\| \leq \max(\varepsilon, \varepsilon^2) \implies \lambda_{\min}(Z) \geq T(1 - \epsilon)^2. \quad (\text{A.1})$$

In the following, we deploy an ϵ -net argument to show the bound on the l.h.s. of (A.1). To this end, let $\{v_\ell\}_{\ell=1}^M$ be an $\frac{1}{4}$ -covering of \mathbb{S}^{n_x-1} . By (Vershynin, 2012, Lemma 5.2) we have $M \leq 9^{n_x}$ and consequently

$$\begin{aligned} \left\| \frac{1}{T_i} Y^\top Y - I \right\| &\leq 2 \max_{\ell \in [1, 9^{n_x}]} \left| v_\ell^\top \left(\frac{1}{T_i} Y^\top Y - I \right) v_\ell \right| \\ &= 2 \max_{\ell \in [1, 9^{n_x}]} \left| \frac{1}{T_i} v_\ell^\top Y^\top Y v_\ell - 1 \right|. \end{aligned}$$

Clearly, for any integer $\ell \in [1, 9^{n_x}]$ we have $v_\ell^\top Y^\top Y v_\ell = \sum_{t=1}^{T_i} v_\ell^\top y_t y_t^\top v_\ell = \sum_{t=1}^{T_i} \zeta_k^2$, where $\zeta_k = v_\ell^\top y_t$ follows a

sub-Gaussian distribution with variance proxy $\sigma_\zeta^2 = 1$. Hence, ζ_k^2 is sub-exponentially distributed with parameters $(4, 4)$, the sum $\sum_{t=1}^{T_i} \zeta_k^2$ is sub-exponentially distributed with parameters $(4T_i, 4)$ and has expected value T_i . Applying the two-sided version of (Wainwright, 2019, Proposition 2.9) with $t = cT_i$, $c \in [0, 1]$, we obtain

$$\begin{aligned} \mathbb{P} [|v_\ell^\top Y^\top Y v_\ell - T_i| \geq cT_i] &= \mathbb{P} \left[\left| \sum_{t=1}^{T_i} \zeta_k^2 - T_i \right| \geq cT_i \right] \\ &\leq \frac{\delta}{9^{n_x}} := 2e^{-\frac{c^2 T_i}{8}}. \end{aligned} \quad (\text{A.2})$$

Observing that

$$|v_\ell^\top Y^\top Y v_\ell - T_i| \geq cT_i \Leftrightarrow \left| \frac{1}{T_i} v_\ell^\top Y^\top Y v_\ell - 1 \right| \geq c,$$

union bounding over all v_ℓ , and solving the right-hand side of (A.2) for a burn-in-time condition, we conclude

$$\left\| \frac{1}{T_i} Y^\top Y - I \right\| \leq 2c \quad (\text{A.3})$$

with probability at least $1 - \delta$ if $T_i \geq \frac{8}{c^2} \log(2 \cdot 9^{n_x}/\delta)$. Combining (A.3) with (A.1) results in the desired result, where we require $c \leq \frac{1}{2}$ for a non-trivial lower bound. \square

The following general result is a direct consequence of Hoeffding's inequality and a covering argument.

Lemma 17 *Let $x_t \stackrel{i.i.d.}{\sim} \text{subG}_{n_x}(\sigma_x^2)$ and fix a failure probability $\delta \in (0, 1)$. Then it holds that*

$$\mathbb{P} \left[\max_{v \in \mathbb{S}^{n_x-1}} \left| v^\top \sum_{t=1}^{T_i} x_t \right| \leq \frac{4}{3} \sigma_x \sqrt{2T_i \log(9^{n_x}/\delta)} \right] \geq 1 - \delta.$$

PROOF. First, we define $\sigma_x y_t = x_t$ such that $y_t \stackrel{i.i.d.}{\sim} \text{subG}_{n_x}(1)$. Note that

$$\max_{v \in \mathbb{S}^{n_x-1}} \left| v^\top \sum_{t=1}^{T_i} x_t \right| = \sigma_x \max_{v \in \mathbb{S}^{n_x-1}} \left| v^\top \sum_{t=1}^{T_i} y_t \right|,$$

i.e., it suffices to analyze

$$\max_{v \in \mathbb{S}^{n_x-1}} \left| v^\top \sum_{t=1}^{T_i} y_t \right| = \left\| \sum_{t=1}^{T_i} y_t \right\|_2. \quad (\text{A.4})$$

Since we cannot evaluate the maximum in (A.4) directly, we approximate the maximum over the sphere by the maximum over an ϵ -cover. To this end, we define \mathcal{N}_ϵ to be an ϵ -net of \mathbb{S}^{n_x-1} . Defining v^* as the maximizer of (A.4) it follows that for some $v_\ell \in \mathcal{N}_\epsilon$ which approximates $v^* = \arg \max_{v \in \mathbb{S}^{n_x-1}} |v^\top \sum_{t=1}^{T_i} y_t|$, such that $\|v_\ell - v^*\| \leq \epsilon$, where $\epsilon \in [0, 1)$, we have

$$\begin{aligned} \left| v_\ell^\top \sum_{t=1}^{T_i} y_t \right| &\geq \left| v^*^\top \sum_{t=1}^{T_i} y_t \right| - \left| (v^* - v_\ell)^\top \sum_{t=1}^{T_i} y_t \right| \\ &\geq (1 - \epsilon) \left\| \sum_{t=1}^{T_i} y_t \right\|_2. \end{aligned} \quad (\text{A.5})$$

Choosing $\epsilon = \frac{1}{4}$ yields with (Vershynin, 2012, Lemma 5.2) that $|\mathcal{N}_\epsilon| \leq 9^{n_x}$, and by (A.5) we obtain

$$\left\| \sum_{t=1}^{T_i} y_t \right\|_2 = \max_{v \in \mathbb{S}^{n_x-1}} \left| v^\top \sum_{t=1}^{T_i} y_t \right| \leq \frac{4}{3} \max_{\ell \in [1, 9^{n_x}]} \left| v_\ell^\top \sum_{t=1}^{T_i} y_t \right|. \quad (\text{A.6})$$

Note that, by construction, $v_\ell^\top y_t \sim \text{subG}(1)$ for any integer $\ell \in [1, 9^{n_x}]$ since $y_t \sim \text{subG}_{n_x}(1)$. Thus, by applying Hoeffding's inequality for each v_ℓ we obtain

$$\mathbb{P} \left[\left| \sum_{t=1}^{T_i} v_\ell^\top y_t \right| \geq \sqrt{2T_i \log(9^{n_x}/\delta)} \right] \leq \frac{\delta}{9^{n_x}}.$$

Taking the union bounding over all $v_\ell \in \mathcal{N}_\epsilon$ yields

$$\mathbb{P} \left[\max_{\ell \in [1, 9^{n_x}]} \left| \sum_{t=1}^{T_i} v_\ell^\top y_t \right| \leq \sqrt{2T_i \log(9^{n_x}/\delta)} \right] \geq 1 - \delta.$$

By (A.6) and (A.4), we deduce

$$\mathbb{P} \left[\max_{v \in \mathbb{S}^{n_x-1}} \left| v^\top \sum_{t=1}^{T_i} x_t \right| \leq \frac{4}{3} \sigma_x \sqrt{2T_i \log(9^{n_x}/\delta)} \right] \geq 1 - \delta$$

which concludes the proof. \square

B Proof of Lemma 10

First, we show that if $x \stackrel{\text{i.i.d.}}{\sim} U(a)$ then $\sin(x)$ is a zero-mean random variable. In particular,

$$\mathbb{E}[\sin(x)] = \int_{-\infty}^{\infty} \sin(x) f_X(x) dx = \frac{1}{2a} \int_{-a}^a \sin(x) dx = 0.$$

Further, observe that $\sin(x) \in [-1, 1]$ for all $x \in \mathbb{R}$ and let $v \in \mathbb{S}^1$ and $\lambda \in \mathbb{R}$. Now, let ε be an independent Rademacher variable.³ Note that since $v^\top \xi$ is symmetric, $v^\top \xi$ and $\varepsilon v^\top \xi$ share the same distribution. Hence,

$$\begin{aligned} \mathbb{E} \left[e^{\lambda v^\top \xi} \right] &= \mathbb{E} \left[\mathbb{E}_\varepsilon \left[e^{\varepsilon \lambda v^\top \xi} \right] \right] \\ &\leq \mathbb{E} \left[e^{\frac{\lambda^2 (v^\top \xi)^2}{2}} \right] = \mathbb{E} \left[e^{\frac{\lambda^2 (v_1 x + v_2 \sin(x))^2}{2}} \right], \end{aligned}$$

where the inequality follows from (Wainwright, 2019, Example 2.3). Since the variance proxy needs to hold for all $v \in \mathbb{S}^1$, we consider

$$\max_{v \in \mathbb{S}^1} v_1^2 x^2 + v_2^2 \sin^2(x) + 2v_1 v_2 x \sin(x).$$

In the following, we crudely bound this by

$$\max_{v \in \mathbb{S}^1} v_1^2 a^2 + v_2^2 + 2a = \max_{v_1 \in [-1, 1]} v_1^2 (a^2 - 1) + 2a + 1.$$

Clearly, this yields

$$\mathbb{E} \left[e^{\lambda v^\top \xi} \right] \leq \begin{cases} e^{\frac{\lambda^2}{2} (2a+1)}, & \text{if } a \in (0, 1], \\ e^{\frac{\lambda^2}{2} (a^2+2a)}, & \text{if } a \in (1, \infty), \end{cases}$$

which concludes the proof. \square

³ A Rademacher variable ε takes the values $\{-1, 1\}$ with equal probability.

C Proof of Proposition 11

We prove Proposition 11 by deriving the quadratic bound in (29) from the individual identification error bounds in (23). To this end, recall the residual $r(x, u)$ in (28) and observe that we can rewrite it as

$$r(x, u) = (1 - \sum_{i=1}^{n_u} [u]_i) \Delta A x + \Delta B_0 u + \sum_{i=1}^{n_u} [u]_i \Delta B_i x, \quad (\text{C.1})$$

where $\Delta A = A - \hat{A}$, $\Delta B_0 = B_0 - \hat{B}_0$, $\Delta B_i = B_i - \hat{B}_i$. Then, the identification error bounds (23) yield

$$\begin{aligned} \|r(x, u)\|_2 &\leq \left| 1 - \sum_{i=1}^{n_u} [u]_i \right| \|\Delta A\|_2 \|x\| + \sqrt{\sum_{i=1}^{n_u} \|[\Delta B_0]_i\|_2^2 \|u\|} \\ &\quad + \sum_{i=1}^{n_u} |[u]_i| \|\Delta B_i\|_2 \|x\| \\ &\leq \left[\max_{u \in \mathbb{U}} \left| 1 - \sum_{i=1}^{n_u} [u]_i \right| \right] \varepsilon_A \|x\| + \sqrt{\sum_{i=1}^{n_u} \varepsilon_{[B_0]_i}^2 \|u\|} \\ &\quad + \left[\max_{u \in \mathbb{U}} \sum_{i=1}^{n_u} |[u]_i| \varepsilon_{B_i} \right] \|x\| \end{aligned}$$

with probability at least $1 - \delta$. Recall c_x, c_u in (31) and observe with probability at least $1 - \delta$ that

$$\|r(x, u)\|_2^2 \leq (c_x \|x\|_2 + c_u \|u\|_2)^2 \leq 2c_x^2 \|x\|_2^2 + 2c_u^2 \|u\|_2^2.$$

This ensures the quadratic bound in (29) with probability at least $1 - \delta$ for Q_Δ as in (30). \square

D Proof of Proposition 12

In the following, we prove Proposition 12 by deriving the quadratic bound in (29) from the ellipsoidal identification error bounds in (26). Based on the representation of the remainder in (C.1), we deduce with probability at least $1 - \delta$

$$\begin{aligned} &\|r(x, u)\|_2^2 \\ &= (\star)^\top \left((1 - \sum_{i=1}^{n_u} [u]_i) \Delta A x + \Delta B_0 u + \sum_{i=1}^{n_u} [u]_i \Delta B_i x \right) \\ &= (\star)^\top \left((1 - \sum_{i=1}^{n_u} [u]_i) \Delta A x + \sum_{i=1}^{n_u} \left[\begin{smallmatrix} \Delta B_i^\top \\ [\Delta B_0]_i^\top \end{smallmatrix} \right]^\top \left[\begin{smallmatrix} [u]_i x \\ [u]_i \end{smallmatrix} \right] \right) \\ &\leq x^\top (n_u + 1) (1 - \sum_{i=1}^{n_u} [u]_i)^2 \Delta A^\top \Delta A x \\ &\quad + \sum_{i=1}^{n_u} (n_u + 1) [\star]^\top [\star] \left[\begin{smallmatrix} \Delta B_i^\top \\ [\Delta B_0]_i^\top \end{smallmatrix} \right]^\top \left[\begin{smallmatrix} [u]_i x \\ [u]_i \end{smallmatrix} \right] \\ &\leq (n_u + 1) \left((1 - \sum_{i=1}^{n_u} [u]_i)^2 x^\top \mathcal{E}_A x + \sum_{i=1}^{n_u} [\star]^\top \mathcal{E}_{B_i} \left[\begin{smallmatrix} [u]_i x \\ [u]_i \end{smallmatrix} \right] \right), \end{aligned}$$

where we exploit the binomial expansion for the penultimate inequality and (26) for the last inequality. Hence,

$$\begin{aligned} &\|r(x, u)\|_2^2 \leq x^\top (n_u + 1) \max_{u \in \mathbb{U}} |1 - \sum_{i=1}^{n_u} [u]_i|^2 \mathcal{E}_A x \\ &\quad + (n_u + 1) [\star]^\top [\star]^\top \hat{\mathcal{E}}_B \begin{bmatrix} (u \otimes I_{n_x}) & 0 \\ 0 & I_{n_u} \end{bmatrix} \begin{bmatrix} x \\ u \end{bmatrix}. \end{aligned}$$

with probability at least $1 - \delta$. Then, defining $\hat{\mathcal{E}}_B$ as in (32b) yields the Q_Δ in (32). \square